Applications of Hierarchical Constellations for Multimedia Transmission over Fading Channels

by

Md. Jahangir Hossain
B. Sc. Engg., Bangladesh University of Engineering and Technology, 2000

A Thesis Submitted in Partial Fulfillment of the Requirements
for the Degree of

MASTER OF APPLIED SCIENCE

in the Department of Electrical and Computer Engineering

We accept this thesis as conforming
to the required standard

[redacted]

Dr. V. K. Bhargava, Supervisor (Department of Electrical and Computer Engineering)

[redacted]

Dr. T. A. Gulliver, Member (Department of Electrical and Computer Engineering)

[redacted]

Dr. S. Dost, Outside Member (Department of Mechanical Engineering)

[redacted]

Dr. J. A. Ellis, External Examiner (Department of Computer Science)

Supervisor: Dr. Vijay K. Bhargava

ABSTRACT

Hierarchical constellations (known also as embedded, multi-resolution, asymmetrical or nonuniform constellations) are studied for multimedia and multicast transmission over fading channels. Specifically, we propose general design guidelines for multimedia and multicast transmission over fading channels using an adaptive hierarchical phase shift key (PSK) constellation. By computer simulation, we have compared our proposed schemes (for both applications) with a classical time division multiplexing (TDM) that employs uniform PSK of the same order as hierarchical PSK. The adaptive hierarchical PSK, generally, outperforms (in terms of energy) the adaptive uniform PSK in TDM.

We also propose a new technique for simultaneous voice and multi-class data transmission over fading channels using adaptive hierarchical M-ary quadrature amplitude modulation (M-QAM). We present closed-form expressions and numerical results for outage probability, achievable spectral efficiency and average bit error rate (BER) for voice and different classes of data transmission over Nakagami-m fading channels. Compared to the schemes employing hybrid binary shift keying (BPSK)/M-ary amplitude modulation (M-AM) and uniform M-ary quadrature amplitude modulation (M-QAM), the new hierarchical scheme is spectrally more efficient for data transmission. The new scheme provides also as a byproduct a spectrally efficient way of transmitting voice and single class data.

Examiners:

[redacted]

Dr. V. K. Bhargava, Supervisor (Department of Electrical and Computer Engineering)

[redacted]

Dr. T. A. Gulliver, Member (Department of Electrical and Computer Engineering)

[redacted]

Dr. S. Dost, Outside Member (Department of Mechanical Engineering)

[redacted]

Dr. J. A. Ellis, External Examiner (Department of Computer Science)

Table of Contents

List of Tables

List of Figures

List of Abbreviations

AM	Amplitude modulation
ARQ	Automatic repeat request
AWGN	Additive white Gaussian noise
BER	Bit error rate
BPSK	Binary phase shift keying
CNR	Carrier-to-noise ratio
dB	Decibel
D-TDMA	Dynamic time division multiple access
DVB-T	Digital video broadcasting - terrestrial
I-ISMA	Idle signal multiple access for integrated service
LSB	Least significant bit
MAC	Media access control
MSB	Most significant bit
OFDM	Orthogonal frequency division multiplexing
PAM	Pulse amplitude modulation
PDF	Probability density function
PMRA	Packet reservation multiple access
PSK	Phase-shift-keying
QAM	Quadrature amplitude modulation
QoS	Quality of service
QPSK	Quadrature phase shift keying
TDM	Time division multiplexing
TDMA	Time division multiple access

W	Watts

Acknowledgement

I would first like to express my gratitude towards my supervisor, Professor Vijay K. Bhargava without whose guidance, attention to detail, financial assistance and encouragement, I could not have completed this work. At the same time, special thanks goes to Dr. Mohamed-Slim Alouini at the University of Minnesota. His initial direction, invaluable suggestions and helpful advice made this work completed so quickly. My sincere thanks are also extended to all my teachers from primary school to university for their guidance.

The friendly and supportive atmosphere inherent to the Communication Group at UVic contributed essentially to the final outcome of my studies. From outside of the group, Pavan, at the University of Minnesota, extended his help by allowing me to use his codes. In this context I would like to thank particularly Ashok, Blazek, Chandika, Catherine, Dejan, Daniela, Mao, Mercier, Olivier, Pom, Pavan and Serkan.

It is not possible to mention all the people that have in some way influenced this work. Specially, all of my friends and my land lady Mrs. Leta Richards at Victoria helped me a lot directly and indirectly to continue my study at UVic. So, I would like to take this opportunity to thank them. Last, but not the least, the biggest personal thanks goes to my family, especially to my parents, my uncles and grandparents.

Dedication

To my beloved parents and to the members of my family whose blessing, love and affection have been the greatest possession in my life

Chapter 1

Introduction

Future generation mobile networks need to support mixed traffic such as voice, facsimile, file transfer, e-mail and Internet access. In general, mixed traffic consists of different messages that require different quality parameters such as delay, data rate and bit error rate (BER). Some typical requirements are given in Table 1.1 [1]. As such, the demand for the mixed traffic over the wireless networks with limited radio spectrum is growing at a rapid pace. Furthermore, in wireless communications, due to the time-varying nature of fading, fixed transmission techniques, which are designed to guarantee a reliable communication even in deep fades suffer from spectral inefficiency. Therefore, new spectrally efficient multimedia communication techniques need to be designed.

Taking advantage of the time-varying nature of wireless channels, a variety of adaptive transmission techniques have been developed to improve system spectral efficiency.

Table 1.1. *Bit error rate and delay requirements of various data types.*

Data Type	BER	Delay	Delay Jitter
Voice	10^{-3}	Critical	Non-Critical
Facsimile	10^{-4}	Non-Critical	Non-Critical
Low Resolution Video	10^{-5}	Non-Critical	Critical
Asynchronous Packet Data	10^{-9}	Non-Critical	Non-Critical
Synchronous Packet Data	10^{-9}	Non-Critical	Critical

These techniques assume that the channel quality is known at both receiver and transmitter. According to the channel quality, these adaptive schemes change various transmission parameters, such as transmitted power level [2], symbol rate [3], coding rate/scheme [4], constellation size [5]-[9], or any combination of these parameters [10]-[15]. Most of these techniques use uniform constellation such as uniform quadrature amplitude modulation (QAM), uniform phase shift key (PSK) and uniform amplitude modulation (AM) and their goal is to improve the link average spectral efficiency ($\langle R \rangle / W$[bits/s/Hz]), defined as the average transmitted data rate per unit bandwidth for a specified average carrier-to-noise ratio (CNR) and BER. Buffering of the input data may be required, since the outage probability of such schemes can be quite high, especially for the channels with low average CNR.

In multicasting scenario where a transmitter needs to transmit message of same quality to a number of recipients in the networks, the adaptation problem is quite different. The recipients are generally located in different physical locations and their channels experience different fading conditions and interference levels. The transmitter, therefore, finds different users with different link qualities. Though the adaptive adaptive schemes, which use uniform constellation discussed above, can improve the system spectral efficiency, it is difficult to use them in multicasting due to the difference in recipients' link qualities. Therefore, the system designer faces difficulty in selecting an efficient modulation scheme for multicasting that is optimized for minimum transmit power and bandwidth while still supporting the required quality parameters of the existing users.

Considerable research efforts have been devoted in recent years for the integration of voice and data for wireline [16] and wireless communication systems [17]-[24]. For the latter systems (e.g., [19]-[24]) these efforts focused on the development of a variety of media access control (MAC) techniques and protocols such as packet reservation multiple access (PMRA), idle signal multiple access for integrated services (I-ISMA), and dynamic time division multiple access (D-TDMA). The proposed schemes, in [17] and [18], offered link layer solution to the voice and data integration problem.

1.1 Significance of Research

One of the contributions of this thesis is the application of hierarchical constellations in generalized multimedia and multicast transmission over fading channels. Specifically, it shows general design guidelines for multimedia and multicast transmission using adaptive hierarchical M-ary phase shift key (M-PSK) constellation. The proposed schemes outperform (in terms of energy) the classical uniform PSK in time division multiplexing (TDM).

The other major contribution of this thesis is a new simultaneous voice and multi-class data transmission technique over fading channels. The new scheme which uses adaptive hierarchical M-ary quadrature amplitude modulation (M-QAM), is spectrally more efficient for data transmission while offering satisfactory voice communication. The closed-form expressions for outage probability, spectral efficiency and average BER have been derived for voice and different kinds of data transmission. The new scheme provides also as a byproduct a spectrally efficient way of transmitting voice and single class data.

1.2 Thesis Outline

This thesis consists of five chapters. Chapter 2 presents the background material of the thesis. Specifically, it presents an overview of the channel model, hierarchical constellations and their BER performances over additive white Gaussian noise (AWGN) channel.

Chapter 3 provides a multimedia and a multicast transmission technique over fading channels using adaptive hierarchical PSK modulation. The performance of the proposed schemes is compared with the schemes employing uniform PSK constellation in TDM.

Simultaneous voice and multi-class data transmission technique using adaptive hierarchical modulation has been described in Chapter 4. We have also extended the schemes in [17] and [18] for simultaneous voice and multi-class data transmission. Assuming perfect channel estimation and negligible time delay, the performances of the new scheme and the extended schemes are analyzed in this chapter. In particular, closed-form expressions for

the outage probability, the achievable spectral efficiency and average BER for voice and data (both classes) transmission are derived. Moreover, these expressions are exploited to evaluate the performance of the voice and single class data transmission using hierarchical M-QAM. Numerical results that allow to compare the behaviors of different schemes under consideration (for simultaneous voice and multi-class data transmission) are also presented in Chapter 4. Chapter 5 then summarizes and concludes the thesis.

Chapter 2

Background

This chapter presents background information on the channel model, hierarchical constellations and the BER performance of these types of constellations over AWGN channel.

2.1 Channel Models

We consider the same channel model that was considered in [17] and [18] i.e., a slowly varying flat-fading channel changing at a rate much slower than the symbol data rate and the channel fading amplitude α is characterized by the Nakagami-m probability density function (PDF) given by [25, Eq. (11)]

$$p_\alpha(\alpha) = 2\left(\frac{m}{\Omega}\right)^m \frac{\alpha^{2m-1}}{\Gamma(m)} \exp\left(-m\frac{\alpha^2}{\Omega}\right), \quad \alpha \geq 0 \tag{2.1}$$

where $\Omega = E(\alpha^2)$ is the average received power, m is the Nakagami fading parameter $(m \geq 1/2)$, $\Gamma(\cdot)$ is the gamma function defined by [26, pp. 942, Eq. (8.310.1)]

$$\Gamma(x) = \int_0^{+\infty} t^{x-1}e^{-t}dt, \quad x \geq 0. \tag{2.2}$$

Given the channel fading amplitude α, a signal power P[W], a signal bandwidth of W[Hz], and a noise power density of N_0 [W/Hz], let us define the CNR $\gamma = \alpha^2 P/N_0 W$. So, the CNR γ is distributed according to a gamma distribution, $p_\gamma(\gamma)$, given by [17]

$$p_\gamma(\gamma) = \left(\frac{m}{\bar{\gamma}}\right)^m \frac{\gamma^{m-1}}{\Gamma(m)} \exp\left(-m\frac{\gamma}{\bar{\gamma}}\right), \quad \gamma \geq 0 \tag{2.3}$$

where $\bar{\gamma}$ is the average CNR. The Nakagami-m distribution is used since it can represent a range of multipath channels via the m parameter [25] of fading on the channel: as m increases the amount of fading on the channel decreases. In particular, the Nakagami-m distribution includes the one-sided Gaussian distribution ($m = 1/2$, which corresponds to worst-case fading) and the Rayleigh distribution ($m = 1$) as special cases. Furthermore, the Nakagami-m distribution closely approximates the Nakagami-q (Hoyt) [25, Eq. (59)] and the Nakagami-n (Rice) [25, Eq. (56)] distributions.

2.2 Hierarchical Constellations

Hierarchical constellations (known also as embedded, multi-resolution, asymmetrical or nonuniform constellations) consist of non-uniformly spaced signal points [27], [28], [29], and offers different degree of protection (i.e., BER) to the transmitted message according to their priorities. These protection levels can be controlled by adjusting a set of constellation parameters describing the relative symbol positions in the constellation. Due to the ability of providing different levels of protection to the bits in the same message symbol, this type of constellation has received a great deal of attention in many applications. Some example of these applications are given below:

1. To give every class a different degree of protection according to its importance in broadcasting channels where broadcasted messages are divided into two or more classes, [27], [28], [29].
2. In digital video broadcasting [28], [30].
3. To support multimedia services by simultaneous transmission of different types of traffic, each with its own quality requirements [31], [32], [33].
4. As a possible application in the DVB-T standard [34] in which hierarchical modulations can be used on OFDM sub carriers.

Recently, Pavan and Alouini derived the exact BERs of generalized pulse amplitude (PAM), QAM and PSK constellations [35], [36], [37], [38]. The details of the derivation can be found in these references. Some important details are described below.

2.2.1 PAM Constellations

2.2.1.1 Generalized Hierarchical M-PAM

A generalized $2/4/8/\cdots/M$-PAM ($M = 2^n$) constellation can be modeled as follows. We assume that there are n streams of data, each of which has a priority (i.e., a target BER). We take one bit from each stream to form a symbol of n bits. The bit from the bit stream with highest priority (i.e., the lowest target BER) is assigned to the most significant position, and as such, is referred to as the most significant bit (MSB). The bit from the bit stream with the second highest priority is assigned the next most significant position and so on until the bit from the bit stream with the lowest priority is assigned the lowest significant position. For example, a generalized 2/4/8-PAM with Karnaugh map style Gray mapping is shown Fig. 2.1. In the figure, the fictitious BPSK constellation (from S_1 to S_2) denoted by the large black circle represents the highest priority (hereafter referred to as first level of hierarchy or sub-channel i_1). The distance d_1 represents the first priority. The fictitious grey symbols (from T_1 to T_4) represent the second level of hierarchy. The distance d_2 represents the second priority (second level of hierarchy or sub-channel i_2). Finally, the actual transmitted symbols (from A to H) represent the third priority (third level of hierarchy or sub-channel i_3). The distance d_3 represents the lowest priority (third level of hierarchy or sub-channel i_3). In general, for M-PAM ($M = 2^n$), the M symbols in the constellation are labeled from the left to the right with integer labels starting from 0 to $M - 1$. Then, we convert the integer labels to their binary form. For ith symbol, let the binary equivalent be $b_i^1 b_i^2 \cdots b_i^n$. The corresponding Gray code of the symbol ($g_i^1 g_i^2 \cdots g_i^n$)

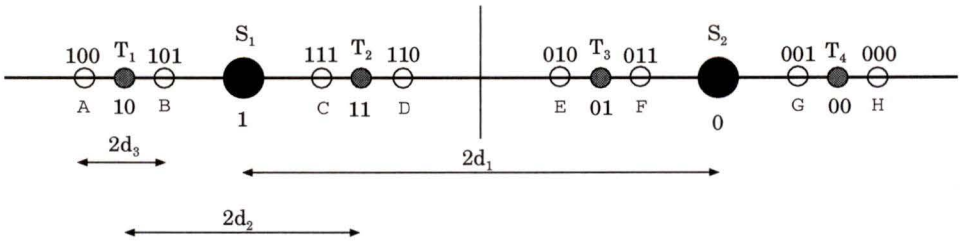

Figure 2.1. *Generalized 2/4/8-PAM constellation.*

$(k = 1, 2, \cdots, n)$ is given by

$$\begin{aligned} g_i^1 &= b_i^1, \\ g_i^k &= b_i^k \oplus b_i^{k-1}, \quad 2 \le k \le n, \quad 1 \le i \le M, \end{aligned} \tag{2.4}$$

where $\oplus$ represents modulo-2 addition.

2.2.1.2 BER Performance

As shown in Fig 2.1, the distances used evolve in a hierarchy. For a generalized hierarchical M-PAM constellation, $2d_1$, $2d_2$, $\cdots$, $2d_{n-1}$ represent distances between points in the first, second, $\cdots$, $(n-1)^{th}$ levels of hierarchy, respectively. Finally, $2d_n$ represents the distance in the final level of hierarchy, where $n = \log_2 M$. The distances can be represented as a vector $\mathbf{d} = [d_1 d_2 \cdots d_n]$ and the corresponding priority vector $\mathbf{p}$ which controls the relative message priority can be expressed as

$$\mathbf{p} = [p_1 p_2 \cdots p_{n-1} p_n] = \left[\frac{d_1}{d_n} \frac{d_2}{d_n} \cdots \frac{d_{n-1}}{d_n} \; 1 \right]. \tag{2.5}$$

The error probability for bit i_k, $P_b(M, \mathbf{d}, i_k)$ of a generalized M-PAM constellation is expressed as [38]:

$$P_b(M, \mathbf{d}, i_k) = \frac{1}{M} \sum_{j=1}^{M} \left[g_j^k + (-1)^{g_j^k} \left[\sum_{l=1}^{2^{k-1}} \frac{1}{2} (-1)^{l+1} \text{erfc} \left[\frac{\mathbf{B}_k(l) - \mathbf{d}_s(j)}{\sqrt{N_0}} \right] \right] \right], \quad k = 1, 2, \cdots, n, \tag{2.6}$$

where

• erfc(·) is complementary error function and given as

$$\text{erfc}(x) = \frac{2}{\sqrt{\pi}} \int_{x}^{+\infty} e^{-t^2} dt, \tag{2.7}$$

• g_j^k (k-th bit in the Gray code of the j-th symbol) has been defined in (2.4).

• $\mathbf{B}_k(\cdot)$ is the vector containing decision boundaries of the k-th bit. It is of size 2^{k-1}, for $k = 1, 2, 3, \cdots, n$. It is defined as follows:

$$\mathbf{B}_k(l) = \frac{\mathbf{d}_s((2l-1)2^{n-k}) + \mathbf{d}_s((2l-1)2^{n-k}+1)}{2}, \quad l = 1, 2, 3, \cdots, 2^{k-1} \tag{2.8}$$

• $\mathbf{d}_s(\cdot)$ is the vector containing the positions of the symbols in the $2/4/\cdots/M$-PAM constellation and is defined as follows:

$$\mathbf{d}_s(j) = \sum_{k=1}^{n} (2b_j^k - 1)d_k, \quad j = 1, 2, \cdots, M, \tag{2.9}$$

where b_j^k is defined in (2.4), and

• $N_0/2$ is the two-sided power spectral density of the AWGN.

The BER expressions in (2.6) can further be expressed as

$$P_b(M, \gamma_{\text{G}}, \mathbf{p}, i_k) = \frac{1}{M} \sum_{j=1}^{M} \left[g_j^k + (-1)^{g_j^k} \left[\sum_{l=1}^{2^{k-1}} \frac{1}{2} (-1)^{l+1} \text{erfc} \left[\frac{\mathbf{D}_k(l) - \mathbf{c}_s(j)}{\sqrt{\mathbf{p}\mathbf{p}^{\text{T}}}} \sqrt{\gamma_{\text{G}}} \right] \right] \right], \quad k = 1, 2, \cdots, n, \tag{2.10}$$

where

• $\mathbf{c}_s(\cdot)$ is defined as follows:

$$\mathbf{c}_s(j) = \sum_{k=1}^{n} (2b_j^k - 1)p_k, \quad j = 1, 2, \cdots, M, \tag{2.11}$$

• $\mathbf{D}_k(\cdot)$ is of size 2^{k-1}, for $k = 1, 2, 3, \cdots, n$. and defined as follows:

$$\mathbf{D}_k(l) = \frac{\mathbf{c}_s((2l-1)2^{n-k}) + \mathbf{c}_s((2l-1)2^{n-k}+1)}{2}, \quad l = 1, 2, 3, \cdots, 2^{k-1} \tag{2.12}$$

- $\gamma_G = E_s/N_0$ is CNR over AWGN channel where

$$E_s = (d_1^2 + d_2^2 + \cdots + d_n^2) = \mathbf{p}\mathbf{p}^T d_n^2. \tag{2.13}$$

2.2.2 QAM Constellations

2.2.2.1 Generalized Hierarchical M-QAM

A generalized hierarchical square M-QAM constellation $(M = 2^{2n})$ can be modeled as follows. We assume that there are n bit streams of data $\left(n = \frac{1}{2}\log_2 M\right)$. Each one of these incoming streams carries information of a particular priority. For every channel access two bits are chosen from each level of priority. The two highest priority bits are assigned the MSB positions in the in-phase (I) and the quadrature phase (Q), respectively. Bits with lower priorities are assigned the subsequent positions of lower significance. For instance the two bits with the second highest priority are assigned the second most significant positions in the I-phase and Q-phase, and so on until the two least priority bits are assigned he LSB position in the I phase and Q phase. This can be viewed as a $4/16/64/\cdots/M$-QAM constellation. For example, a generalized hierarchical 4/16/64-QAM is shown in Fig. 2.2. In the figure, the black and grey symbols are fictitious symbols representing the first and second level of hierarchy, respectively. Finally, the actual transmitted symbols denoted by white circle represent the third level of hierarchy. In the case where every level of priority is not restricted to two bits per channel access, many other QAM constellation can arise. Some examples of of these type constellation, called nonsquare QAM, are given in [35].

2.2.2.2 BER Performance

In general, for M-QAM constellation $(M = 2^{2n})$, there are two sets of distances: one for I phase $(\mathbf{d}^i)$ and the other for Q phase $(\mathbf{d}^q)$ channel. The two distance vectors can be represented as:

$$\mathbf{d}^i = [d_1^i,\ d_2^i \cdots,\ d_n^i] \tag{2.14}$$

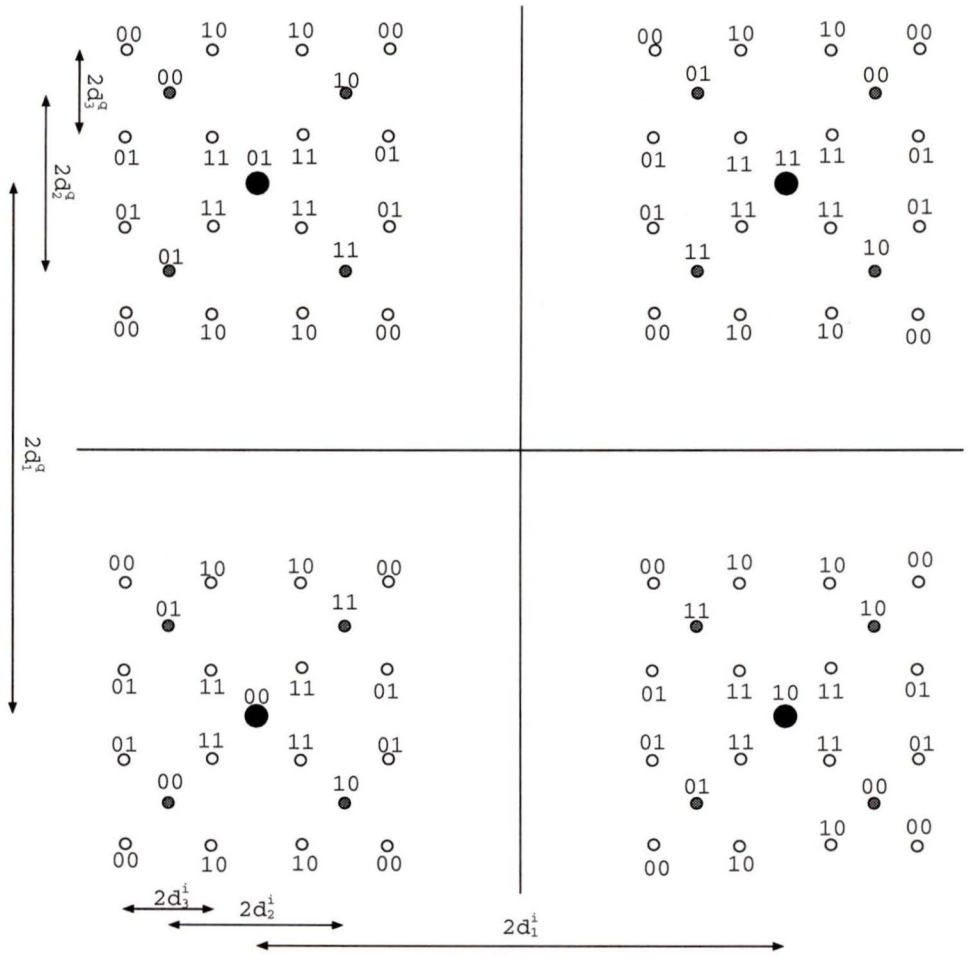

Figure 2.2. *Generalized 4/16/64-QAM constellation.*

and

$$\mathbf{d}^q = [d_1^q,\ d_2^q,\ \cdots,\ d_n^q]. \tag{2.15}$$

Assuming $d_n^i \leq d_n^q$ without loss of generality, corresponding priority vectors are given as

$$\mathbf{p}^i = \left[\frac{d_1^i}{d_n^i},\ \frac{d_2^i}{d_n^i}, \cdots,\ 1\right] \tag{2.16}$$

and

$$\mathbf{p}^q = \left[\frac{d_1^q}{d_n^i},\ \frac{d_2^q}{d_n^i}, \cdots,\ \frac{d_n^q}{d_n^i}\right]. \tag{2.17}$$

The BER of the in-phase bits of square QAM, $P_b^s(M, \gamma_{\mathrm{G}}, \mathbf{p}^i, \mathbf{p}^q, i_k)$ can be written as [35]

$$P_b^s(M, \gamma_{\mathrm{G}}, \mathbf{p}^i, \mathbf{p}^q, i_k) = P_b(\sqrt{M}, \gamma_{\mathrm{G}}, \mathbf{p}^i, i_k), \quad k = 1, 2. \cdots, \tfrac{1}{2}\log_2 M \tag{2.18}$$

where $P_b(\cdot, \cdot, \cdot, \cdot)$ is described in (2.10). The BER of the quadrature phase bits of square QAM, $P_b^s(M, \mathbf{p}^i, \mathbf{p}^q, i_k)$ can be written as [35]

$$P_b^s(M, \gamma_{\mathrm{G}}, \mathbf{p}^i, \mathbf{p}^q, q_k) = P_b(\sqrt{M}, \gamma_{\mathrm{G}}, \mathbf{p}^q, i_k), \quad k = 1, 2. \cdots, \tfrac{1}{2}\log_2 M \tag{2.19}$$

For nonsquare (e.g., rectangular) M-QAM ($M = 2^{2n+1}$), the BER of the in-phase bits $P_b^r(M, \mathbf{p}^i, \mathbf{p}^q, i_k)$ can be written as [35]

$$P_b^r(M, \gamma_{\mathrm{G}}, \mathbf{p}^i, \mathbf{p}^q, i_k) = P_b(\sqrt{2M}, \gamma_{\mathrm{G}}, \mathbf{p}^i, i_k), \quad k = 1, 2. \cdots, \tfrac{1}{2}\log_2 2M \tag{2.20}$$

The BER of the quadrature phase bits of nonsquare QAM, $P_b^r(M, \mathbf{p}^i, \mathbf{p}^q, q_k)$ can be written as [35]

$$P_b^r(M, \gamma_{\mathrm{G}}, \mathbf{p}^i, \mathbf{p}^q, i_k) = P_b(\sqrt{M/2}, \gamma_{\mathrm{G}}, \mathbf{p}^i, q_k), \quad k = 1, 2. \cdots, \tfrac{1}{2}\log_2 \tfrac{M}{2} \tag{2.21}$$

The uniform QAM constellation is a special case of the generalized hierarchical square QAM when $\mathbf{p} = \mathbf{p}^i = \mathbf{p}^q = [2^{n-1}2^{n-2} \cdots 4\ 2\ 1]$. So, the average BER of uniform square QAM can be obtained by averaging the BER performance of the all the bits. Similarly, the uniform rectangular QAM is also special case of hierarchical rectangular QAM when

$$\mathbf{p}^i = [2^n 2^{n-1} \cdots 4\ 2\ 1] \tag{2.22}$$

and

$$\mathbf{p}^q = [2^{n-1}2^{n-2}\cdots 4\ 2\ 1] \tag{2.23}$$

and their BER performance can be obtained by averaging the BER of all the bits.

For example, the analytical plot of the BER expressions for a generalized 4/16/64-QAM is shown in Fig. 2.3 where we have assumed that $\mathbf{p}^i = \mathbf{p}^q = \mathbf{p} = [5\ 2.2\ 1]$. Since we used same priority vector for both $\mathbf{p}^i$ and $\mathbf{p}^q$, the BER performance for Q-phase bit (q_k) is identical to the corresponding I-phase bit (i_k). From Fig. 2.3, it is important to note that to achieve the same target BER for each bit in the transmitted symbol, three sub-channels of hierarchical 4/16/64-QAM require three different CNRs. In other words, for a given CNR, three sub-channels have three different BER performance. This is expected due to the construction of hierarchical QAM constellation. Analytical plots of different position bits of a generalized 4/16/64-QAM for three different priority vectors ($\mathbf{p}^i = \mathbf{p}^q = \mathbf{p} = [10\ 3\ 1]$, $[4\ 2\ 1]$ and $[5\ 2.35\ 1]$) are shown in Figs. 2.4-2.6. These figure show that the protection level (i.e., BER performance) of a given position bit is controlled by the priority vector $\mathbf{p}$.

2.2.3 PSK Constellations

2.2.3.1 Generalized Hierarchical M-PSK

For an example, a generalized hierarchical 2/4/8-PSK is shown in Fig. 2.7 with style Gray mapping. In the figure, the fictitious BPSK constellation denoted by the "$\times$" symbol represents the highest priority (hereafter referred to as first level of hierarchy or sub-channel i_1). The fictitious symbol denoted by "+" at an angle θ_1 represents the second priority (second level of hierarchy or sub-channel i_2). Finally, the Gray labeled circular actual transmitted symbol at an angular distance of θ_2 from the "+" marked symbol, represents the third priority (third level of hierarchy or sub-channel i_3). In other words, the constellation (A through H) can be visualized as a BPSK (S_1 and S_2) embedded in a quadrature phase shift keying (QSPK) (T_1 through T_4), which is further embedded in an 8-PSK (A through H).

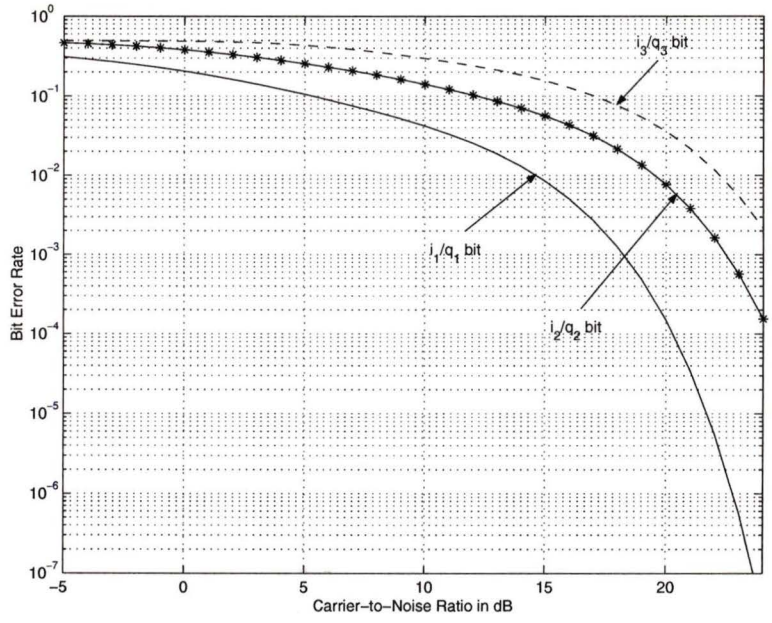

Figure 2.3. *BER of 4/16/64-QAM obtained by setting* $\mathbf{p} = \mathbf{p}^i = \mathbf{p}^q = [5 \;\; 2.2 \;\; 1]$.

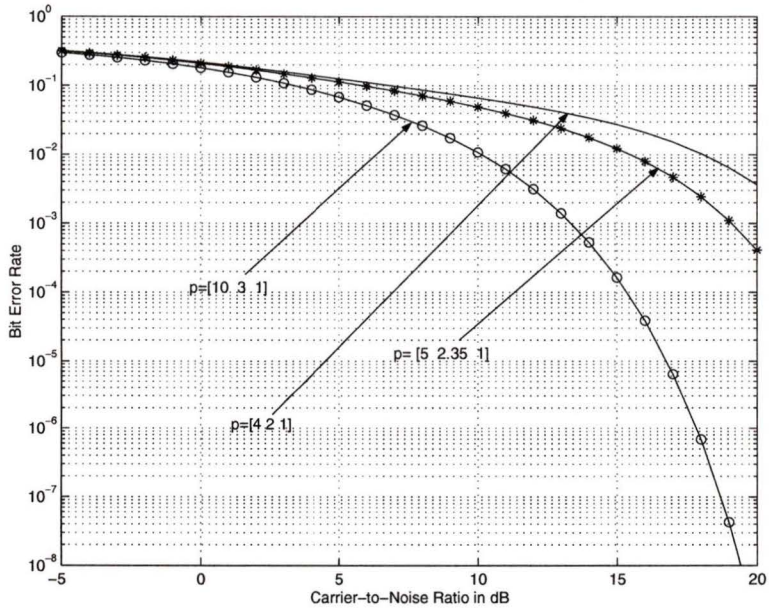

Figure 2.4. *Effect of* $\mathbf{p}$ *on the BER (most significant bit of generalized 4/16/64-QAM).*

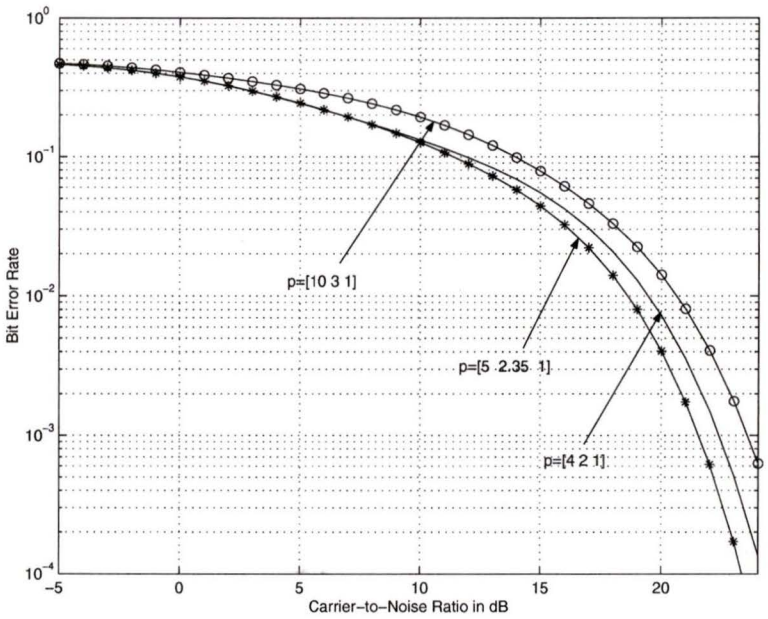

Figure 2.5. *Effect of* **p** *on the BER (middle bit of generalized 4/16/64-QAM).*

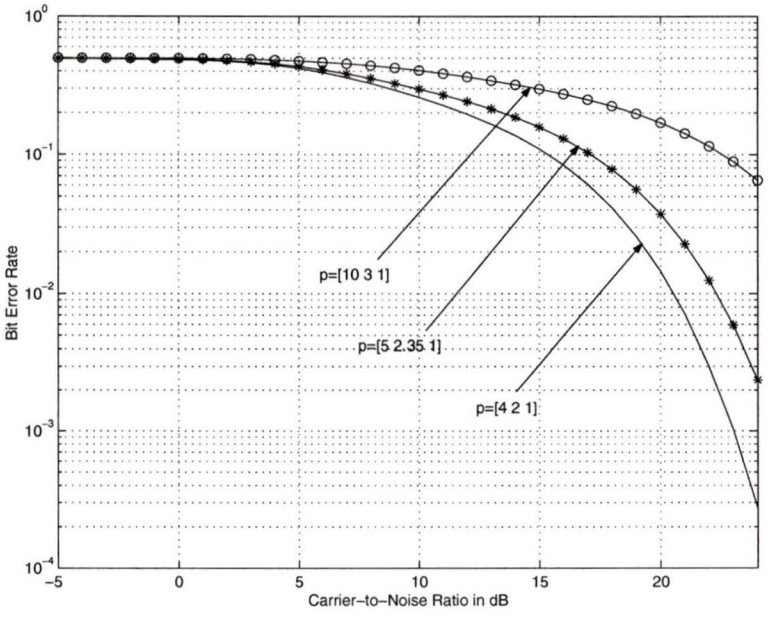

Figure 2.6. *Effect of* **p** *on the BER (least significant bit of generalized 4/16/64-QAM).*

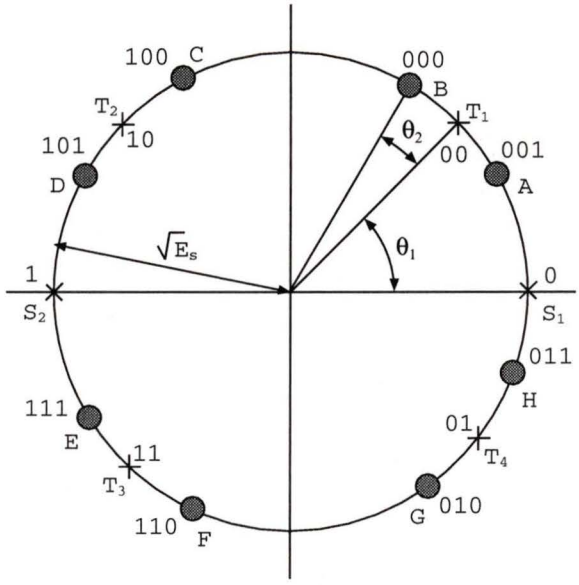

Figure 2.7. *2/4/8-PSK constellation.*

The Gray code of the symbol is obtained by the same procedure as described for the PAM constellation.

2.2.3.2 BER Performance

As shown in Fig. 2.7, the angles used evolve in a hierarchy. For a generalized hierarchical M-PSK constellation, $2\theta_1, 2\theta_2, \ldots, 2\theta_{n-2}$, represent angles between points in the second, third, ..., $(n-1)^{th}$ levels of hierarchy respectively. Finally, $2\theta_{n-1}$ represents the angle in the final level of hierarchy, where $n = \log_2 M$. The angles can be represented as a vector $\boldsymbol{\theta} = [\theta_1 \theta_2 \ldots \theta_{n-1}]_{1\times(n-1)}$. Corresponding priority vector $\mathbf{p}$ becomes

$$\mathbf{p} = [p_1 p_2 \ldots p_{n-1}] = \left[\frac{\theta_1}{\theta_{n-1}} \frac{\theta_2}{\theta_{n-1}} \cdots \frac{\theta_{n-2}}{\theta_{n-1}} \; 1\right] \tag{2.24}$$

The BER of bit i_k in a 2/4/8$\cdots/M$-PSK constellation, $P_b(M, E_s, N_0, \boldsymbol{\theta}, i_k)$, is given by

[37]

$$
\begin{aligned}
P_b(M, E_s, N_0, \boldsymbol{\theta}, i_1) &= \frac{1}{M}\sum_{j=1}^{M}(1-2g_j^1)[-F(\pi-\boldsymbol{\phi}(j))+F(\boldsymbol{\phi}(j))], \\
P_b(M, E_s, N_0, \boldsymbol{\theta}, i_k) &= \frac{1}{M}\sum_{j=1}^{M}(1-2g_j^k)\sum_{l=1}^{2^{k-1}}[-F(\pi-\boldsymbol{\phi}(j))+F(\boldsymbol{\phi}(j))], \\
& \qquad k=2,3,\cdots,n
\end{aligned} \tag{2.25}
$$

where

- g_j^k (k-th bit in the Gray code of j-th symbol) has been defined in (2.4)
- $\mathrm{F}(\cdot)$ is Pawula F-function and defined as [39]

$$
\mathrm{F}(\psi) = -\frac{\mathrm{sgn}(\psi)}{2\pi}\int_0^{\pi-|\psi|}\exp\left[-\gamma_{\mathrm{G}}\frac{\sin^2\psi}{\sin^2\theta}\right]d\theta, \qquad -\pi<\psi<\pi \tag{2.26}
$$

  where $\mathrm{sgn}(\cdot)$ is the sign function and $\gamma_{\mathrm{G}} = E_s/N_0$ is the symbol CNR over AWGN channel.

- $\mathbf{B}_k(\cdot)$ is the vector containing decision boundaries of the k-th bit. It is defined as follows:

  For $k=1$,

$$
\mathbf{B}_1(1) = \pi, \quad \mathbf{B}_1(2) = 0. \tag{2.27}
$$

  For $k=2,3,\cdots,n$, $\mathbf{B}_k(\cdot)$ is of size 2^{k-1}, and is given by

$$
\mathbf{B}_k(l) = \frac{\boldsymbol{\phi}((2l-1)2^{n-k}) + \boldsymbol{\phi}((2l-1)2^{n-k}+1)}{2}, \qquad l=1,2,3,\cdots,2^{k-1} \tag{2.28}
$$

- $\boldsymbol{\phi}(\cdot)$ is the vector containing the positions of the symbols in the $2/4/\cdots/M$-PSK constellation and is defined by:

$$
\boldsymbol{\phi}(j) = \pi + \sum_{k=1}^{n}(2b_j^k-1)\theta_k, \quad j=1,2,\cdots,M, \tag{2.29}
$$

  where b_j^k has been defined prior to (2.4).

As in uniform constellation, the message symbols are uniformly spaced, the angle vector of uniform M-PSK can be represented by

$$\boldsymbol{\theta} = \left[\frac{\pi}{4}\frac{\pi}{8}\cdots\frac{\pi}{M}\right]. \tag{2.30}$$

This is a special case of generalized M-PSK and the average BER is obtained by averaging the BERs of all the bits, i_k $(k = 1, 2, \ldots, \log_2 M)$ [36].

For example, the analytical plot of BER expressions for a generalized 2/4/8-PSK is shown in Fig. 2.8 where we assumed that angle vector $\boldsymbol{\theta} = [\pi/2\ \pi/5\ \pi/12]$. From this figure, it is also evident that the BER performance of different position (sub-channel) bits is different. This is again expected due to the construction of hierarchical PSK constellation. Analytical plots of different position bits of generalized 2/4/8-QAM for three different angle vectors ($\boldsymbol{\theta} = [\pi/2\ \pi/4\ \pi/8]$, $[\pi/2\ \pi/5\ \pi/12]$ and $[\pi/2\ \pi/7\ \pi/15]$) are shown in Figs. 2.9-2.11. These figures show that the BER performance of different position bits is controlled by the angle vector $\boldsymbol{\theta}$.

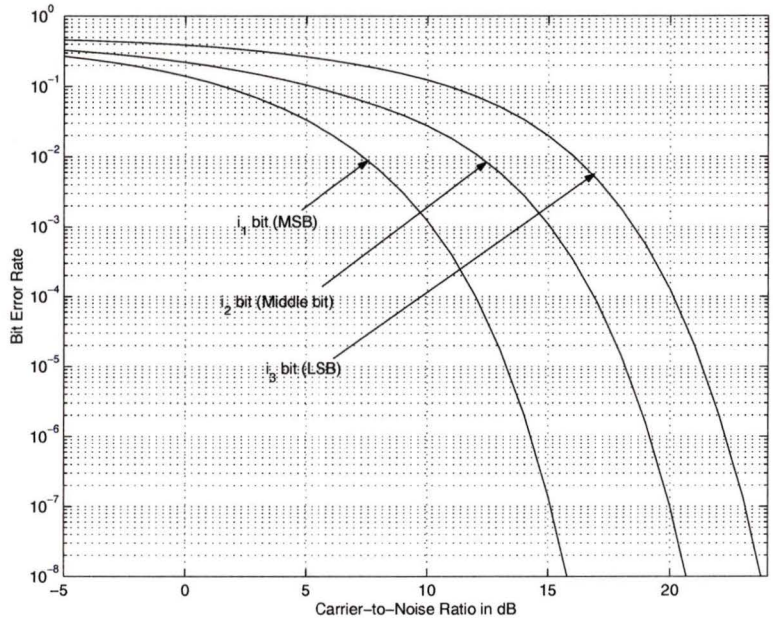

Figure 2.8. *BER of 2/4/8-PSK obtained by setting* $\boldsymbol{\theta} = [\pi/2,\ \pi/5,\ \pi/12]$.

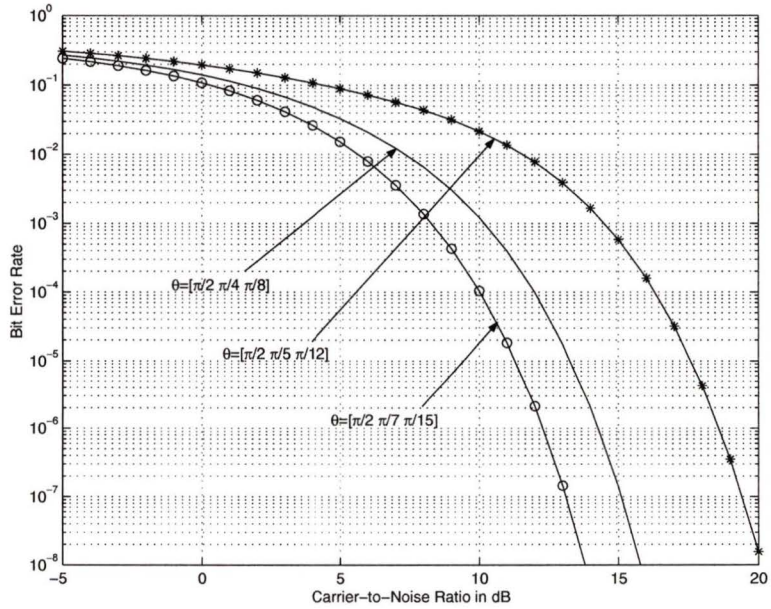

Figure 2.9. *Effect of* $\boldsymbol{\theta}$ *on the BER (most significant position bit of generalized 2/4/8-PSK).*

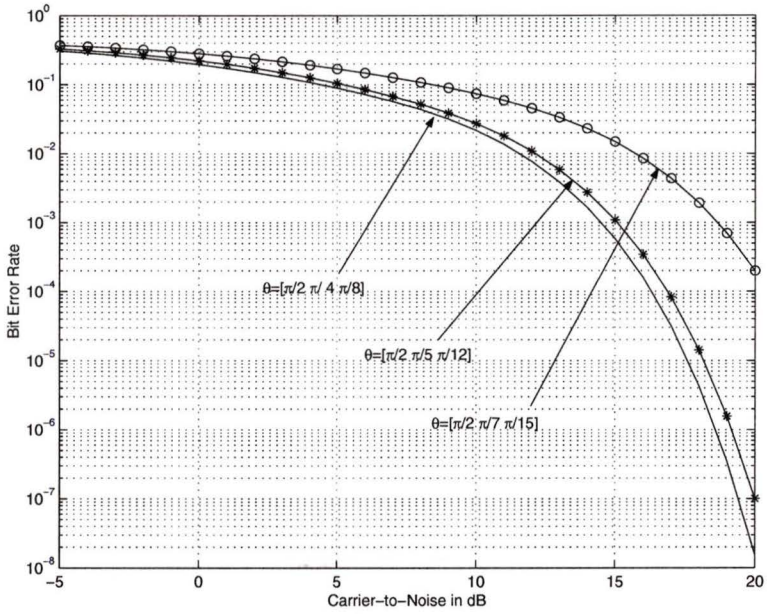

Figure 2.10. *Effect of θ on BER (middle bit of generalized 2/4/8-PSK).*

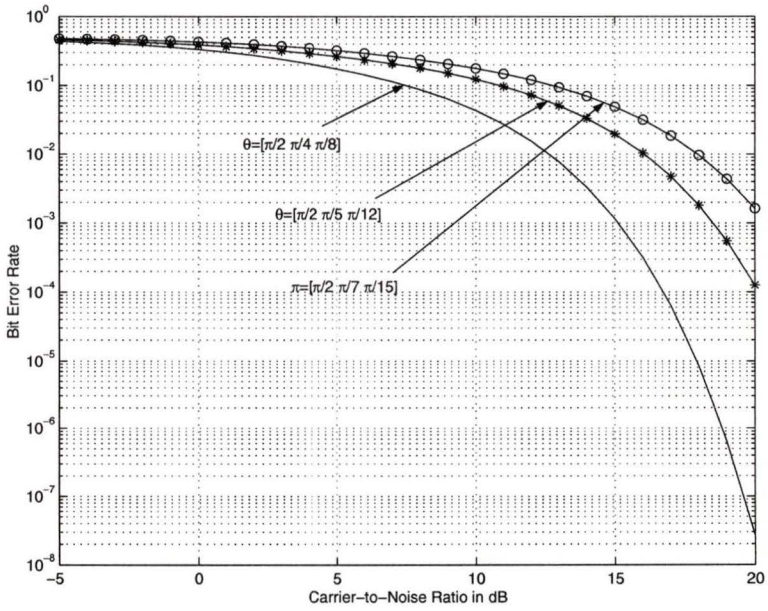

Figure 2.11. *Effect of θ on BER (least significant bit of generalized 2/4/8-PSK).*

Chapter 3

Multimedia and Multicasting

As we described in Chapter 1, nonuniform constellations were studied before to transmit multimedia services in wireless networks as well as in multicasting environments. Specifically, to increase the throughput of the additional message, nonuniform PSK constellations were shown to be effective in transmission of two different classes of message; the basic message and the additional message [33]. In this case, the considered nonuniform M-PSK constellations were derived from uniform PSK constellations of order $N = M/2$. More specifically, they consisted of two parts: a coarse modulation part and a fine modulation part. The coarse modulation part of nonuniform M-PSK, which was selected by one bit of the basic message and $n-2$ bits of the additional message, was essentially a uniform PSK of alphabet size $N = 2^{n-1}$. The error probabilities of these $n-1$ bits sent with coarse modulation, therefore, are approximately equal. The final bit of the additional message was used to determine the fine modulation part of nonuniform M-PSK. The probability of bit error for the bit sent via the fine modulation can be different than that of bits sent with coarse modulation. So, this type of nonuniform PSK constellations were capable of handling messages only at two different error probabilities. The relative values of the two error probabilities were controlled by only one parameter θ called the phase offset. In order to maximize the throughput of additional message, the phase offset θ was proposed to change according to the estimated CNR.

In multicasting environments, the extra capacities of more capable receivers were used to receive multimedia services using nonuniform PSK constellations [32]. The basic multi-

casted message stream was mapped to the constellation points that were far apart in distance from each other than the additional data stream was further mapped to. So, the less capable receiver was able to receive only the basic multicast while the more capable receiver was receiving both the multicasted message as well as the additional message.

In this chapter, at first we capitalize on the concepts of generalized hierarchical PSK constellations and their exact BER expressions developed in [35], [36], [38] to propose a more generalized multimedia transmission technique which is capable of handling more than two different classes of data, each with its own quality requirements. Then in Section 3.2.1, an adaptive hierarchical PSK constellation for multicasting is proposed. In contrast to the scheme proposed in [32], which uses the nonuniform PSK to transmit multimedia multicasting, the goal of the new adaptive scheme proposed for multicasting is to provide different levels of protection to the recipients' links according to their priorities (i.e., qualities). Finally, Section 3.3 presents some examples and simulation results for both multimedia and multicasting over a Rayleigh fading channel.

3.1 Multimedia Transmission

3.1.1 Uplink Transmission

To generalize the problem of transmitting multimedia services on an uplink, let us consider that a mobile transmitter needs to transmit K classes of service. Each class of service S_k $(k = 1, 2, \ldots K)$, has its own required quality parameters i.e., delay constraint, BER Pe_k, data rate $R_k = r_k \times R_b$, where r_k is an integer and R_b is the basic transmission rate which can be obtained by transmitting only one bit in each symbol. Without loss of generality, we assume that $Pe_1 > Pe_2 > \cdots > Pe_K$ and prioritize the service classes according to their required BERs. For example, the lower the required BER is, the higher the priority is. As we described in Chapter 2 that the hierarchical PSK provides different levels of protection to the bits on different sub-channels of a symbol, we exploit this behavior to transmit bits

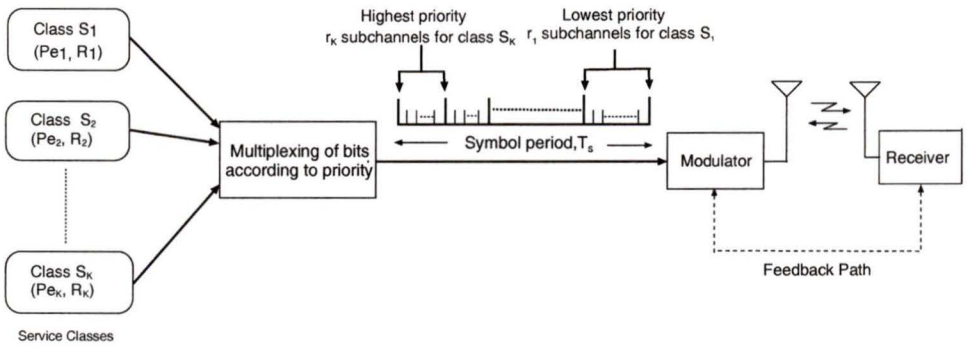

Figure 3.1. *Bit multiplexing with hierarchical constellations for multimedia transmission over wireless fading channels.*

from different classes of service in the same message string.

The block diagram of our proposed adaptive scheme for multimedia transmission is shown in Fig. 3.1. Assuming perfect channel quality N_0' (includes interference, noise, and fading) at the handset and constant N_0' over hundreds of symbols period (i.e., slow fading and/or interference conditions), we describe the details of our proposed system in two steps. First, depending on the required rates r_k $(k = 1, 2, \ldots, K)$ of services the transmitter picks up the alphabet size M, such as n $(= \log_2 M)$ is equal to $\sum_{k=1}^{K} r_k$ and then n sub-channels are assigned to different classes of service according to their required BERs and data rates. Specifically, r_K bits from the highest priority service class S_K, are assigned to r_K successive sub-channels starting from the most significant position sub-channel and so on until the r_1 bits from the lowest priority service class S_1, are assigned to r_1 successive sub-channels ending at the least significant position sub-channel as shown in Fig. 3.1. The symbol period T_s, shown in Fig. 3.1, is equal to $(1/R_b) \log_2 M$. Second, according to estimated N_0', the angles θ_j $(j = 1, 2, \ldots, n-1)$ and E_s are adjusted such as the bits assigned to different sub-channels are sent below their respective required BERs using hierarchical M-PSK over AWGN channel. Since the BER expressions in (2.25) are

not invertible, the parameters E_s and $\boldsymbol{\theta}$ in (2.25) are numerically optimized such as

$$\begin{aligned}
\frac{1}{r_1}\sum_{k=1}^{r_1} P_b(M,\boldsymbol{\theta},E_s,N_0',i_k) &\leq Pe_1,\\
\frac{1}{r_2}\sum_{k=r_1+1}^{r_1+r_2} P_b(M,\boldsymbol{\theta},E_s,N_0',i_k) &\leq Pe_2,\\
&\vdots\\
\frac{1}{r_K}\sum_{k=r_{K-1}+1}^{\log_2 M} P_b(M,\boldsymbol{\theta},E_s,N_0',i_k) &\leq Pe_K.
\end{aligned} \tag{3.1}$$

3.1.2 Downlink Transmission

The downlink transmission is same as the uplink transmission as described in Section 3.1.1. In this case, we assume that there is a reliable reverse link from mobile unit to base station so that the measured value of N_0' at the handset is sent to the base station so that it is used in adapting the downlink transmission parameters in similar fashion described for the uplink transmission.

3.1.3 Comparison with Uniform PSK

To compare the proposed technique with a classical technique, we consider the transmission of services S_k $(k = 1, 2, \ldots K)$, using uniform M-PSK. The uniform M-PSK constellations, which consist of uniformly spaced M signal points, are used to provide roughly same average BER for all the bits transmitted in a symbol. Therefore, the message bits requiring same BER i.e., the bits from same class of service are sent in the same message symbol. Time division multiplexing is used to transmit different classes of service i.e., bits from different services are sent in different time slots. For example, a TDM frame employing uniform M-PSK is shown in Fig. 3.2. Since the modulation order is M, the duration of a time slot, in Fig. 3.2, is equal to symbol duration $T_s = (1/R_b)\log_2 M$ seconds. The required rates of the service classes are provided by assigning appropriate number of time slots in each TDM frame. For instance, the service class S_k are assigned r_k successive

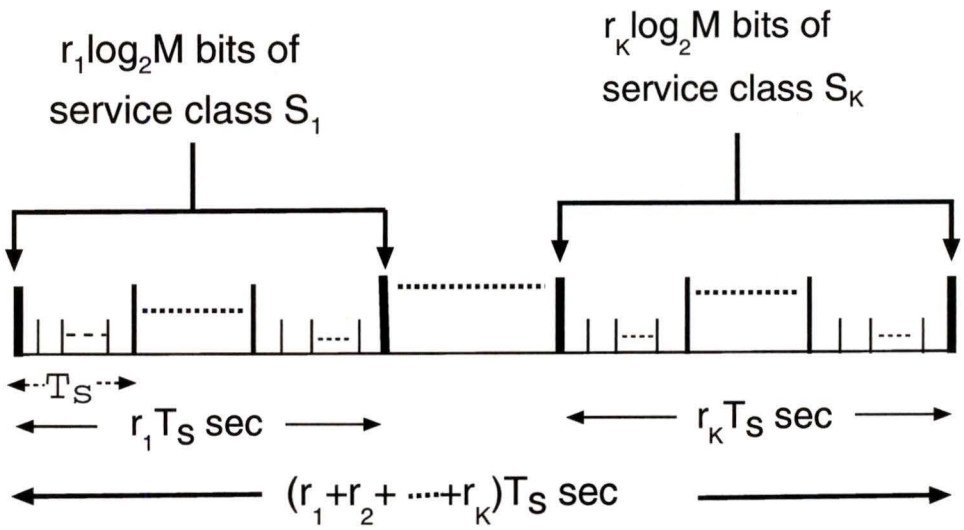

Figure 3.2. *TDM frame structure*

time slots in each frame which contains $\sum_{k=1}^{K} r_k$ time slots as shown in Fig. 3.2. Since the employed modulation scheme is uniform, only the symbol energy E_s is changed according to the estimated channel quality N_0'. More specifically, the transmitter adjusts the transmitted power or equivalently symbol energy E_s in each time slot (i.e., symbol) such as the bits in the symbol are sent below the required BER of service class from which the bits are sent using uniform M-PSK over AWGN channel. Due to time division multiplexing, it introduces extra delay and this delay depends on the number of service classes (K) to be transmitted as well as the required rates of the services r_k $(k = 1, 2, \ldots, K)$.

3.2 Downlink Multiplexing/Multicasting

3.2.1 Downlink Multiplexing/Multicasting

In mobile wireless communication networks, it is a common scenario that a transmitter needs to transmit a message simultaneously to a number of users in the network. In multicasting, for example, radio station transmits a message to a number of recipients. But these

users' communication links may have different interference levels, fading conditions and/or noise levels. Thus different recipients have different link qualities. In general, we consider that there are n recipients in a wireless network to receive a message with a required data rate of R_b, BER of Pe and specified delay. For a fixed transmit power, reliability (i.e., BER) of the received message of these recipients depends on their individual instantaneous link quality N_0' (includes interference, noise, and fading). The better the link quality, the more reliable the received message is and vice-versa. If the instantaneous link qualities N_{0_i}' $(i = 1, 2 \ldots, n)$ are known to the transmitter, the recipients' links can be ranked from the more reliable link to the less reliable link. For example, the recipient with the lowest value of N_0' has the most reliable channel and so on. Therefore, to receive message of same reliability, the least reliable link requires the most protection and so on. As hierarchical PSK provides more protection to the most significant bit (MSB) than the least significant bit (LSB) by virtue of Gray coding, the least protected sub-channel can be assigned to the most reliable link, the next protected sub-channel to the next reliable link and so on until the most protected sub-channel is assigned the least reliable link. Then the transmitter will adjust the transmitted symbol energy E_s and the angle vector $\boldsymbol{\theta}$ such that all the m bits are sent below the required BER Pe using hierarchical PSK of alphabet size $M = 2^n$ over AWGN channel. In our following proposed algorithm, we refer the adjusted parameters for a given set of N_{0_i}' $(i = 1, 2 \ldots, n)$ as optimum transmission parameters. Assuming a perfect channel quality estimation and slow fading condition, we propose the following adaptation algorithm:

1. The transmitter at the base station knowing all the link status N_{0_i}' $(i = 1, 2, \ldots, n)$, ranks the links according to their qualities and assigns them different sub-channels, accordingly. With this assignments, the transmitter tries to find the optimum transmission parameters for hierarchical M-PSK within a certain period of time which is determined by the delay requirement of the service. If it finds the optimum transmission parameters, it transmits the message symbol from the hierarchical PSK constellation according to these optimum parameters.

2. If the base station does not find the optimum parameters within the specified time, it transmits the message symbol from the uniform M-PSK constellation. In this case, rather than transmitting one bit for each recipient in a symbol as with hierarchical M-PSK, all the $\log_2 M$ bits in the symbol is transmitted for same recipient and the symbol energy E_s is adjusted according to the corresponding recipient's link quality to achieve the target BER Pe using uniform M-PSK over AWGN channel. After sending one symbol for each recipient from uniform PSK constellation, the scheme again repeats from Step 1.

The number as well as the position(s) of the bit(s) in the transmitted symbol for an individual recipient's are sent via feedforward channel from the base station to the recipient's unit. Thus the recipients receive the symbol and look only for the bit(s) in the particular position(s) in each received symbol.

3.2.2 Comparison with Uniform PSK

Uniform PSK with time division multiplexing can also be used to transmit message of same quality to a number of users. To compare the proposed scheme in Section 3.2.1 with uniform PSK in TDM, we consider the transmission of a message with a required rate of R_b and BER of Pe to n recipients having the link quality N'_{0_i} $(i = 1, 2, \ldots, n)$ as described in Section 3.2.1. Rather than assigning different sub-channels to different recipients, different time slots are assigned to different recipients. Specifically, each recipient is assigned one time slot in each TDM frame, which contains n time slots, to provide all recipients the same average data rate R_b. The duration of a time slot is equal to symbol duration $T_s = (1/R_b) \log_2 M$. The transmitted power or equivalently the symbol energy E_s in each time slot (i.e., symbol) is controlled such as the bits are sent below the required BER Pe at the measured value of N'_0 in the corresponding time slot using uniform M-PSK over AWGN channel.

3.3 Simulation Results and Discussion

In this section we present some numerical examples and simulation results for both multimedia transmission and multicasting. In our simulation, we consider a slowly varying Rayleigh flat-fading channel (i.e., $m = 1$ in (2.3)) changing at a rate much slower than the symbol data rate, so the channel remains roughly constant over hundreds of symbols. We use the MATLAB Statistics Toolbox and Optimization Toolbox. We assume that the channel quality N_0' is known to the transmitter. In multicasting, it is assumed that the intended recipients have complete knowledge about the positions of their bits in multicasted symbol.

3.3.1 Multimedia Transmission

We have considered simultaneous transmission of two different classes of service. The required data rates as well as the required BER for these services are given in Table 3.1. The gains with the proposed scheme employing hierarchical 8-PSK over the adaptive uniform 8-PSK in TDM are given in Table 3.1 for different combinations of service classes. The angles θ_1 and θ_2 of the angle vector $\boldsymbol{\theta}$ for different cases are also listed in Table 3.1. From the table, it is evident that the gain depends on the services transmitted. As the difference between BER requirements of two different class of services increases, the gain also increases. For example, the gains for service class S_1 (average BER$= 10^{-2}$) with service class S_3 (average BER$= 10^{-4}$), S_4 (average BER$= 10^{-5}$) and S_5 (average BER$= 10^{-6}$) are 0.6880 dB, 0.9497 dB and 1.1369 dB, respectively. The gain comes from the relative protection level obtained by adjusting the angle vector $\boldsymbol{\theta}$. Actually, the Gray coded uniform PSK also provides different degree of protection to the bits transmitted on different positions of a symbol. But the relative protection level can not be adjusted according to requirements as the angle vector $\boldsymbol{\theta}$ is fixed. So, the different levels of protection provided by uniform PSK, can not be exploited to transmit bits requiring different BERs in the same message symbol. Roughly the same average BER are provided to all the bits in a message symbol where the average BER of uniform PSK is dominated by the BER of the least pro-

tected sub-channel. So, as the difference of BER requirements between different service classes increases, the gain also increases. For example, at 14.75 dB CNR, the uniform 8-PSK provides BERs of 7.76×10^{-4} in the MSB, 7.76×10^{-4} in the next significant bit and 1.55×10^{-3} in the LSB. Thus the average BER is 1.03×10^{-3}. At the same CNR, hierarchical 8-PSK with $\boldsymbol{\theta} = [0.7644\ 0.3052]$ provides BERs of 5.13×10^{-5} in the MSB, 1.54×10^{-4} in the next significant bit and 1.01×10^{-2} in the LSB. Thus the average BER of the two most priority bits is 10^{-4} which is the required average BER of service class S_3 as shown in Table 3.1. The listed angles show that the angle vector $\boldsymbol{\theta}$ depends only on the transmitted services. It is obvious from the discussion and (2.25) that the vector $\boldsymbol{\theta}$ controls the relative protection level of the bits on different sub-channels. To provide a relative protection level, the vector $\boldsymbol{\theta}$ is fixed for any link condition and only the parameter symbol energy E_s is changed according to the link quality N_0'. So, the adaptation process for multimedia transmission proposed in Section 3.1.1 becomes easier and can be done only by adjusting the E_s according to measured value of N_0' as long as the required QoS parameters of the services are same. Only at the beginning of first transmission of given service classes, the angles θ_j $(j = 1, 2, \ldots, n-1)$ should be adjusted according to the required quality parameters of the services.

3.3.2 Multicasting

We have considered that three recipients are receiving message from a base station with a data rate of R_b and BER of 10^{-3}. The proposed multicasting technique with hierarchical 8-PSK provides different gains for different combinations of link qualities. Gains for some combinations are shown in Table 3.2 as examples. Example 11 and 14 in Table 3.2 show a gain of 0 dB. In these cases, the optimum transmission parameters using the hierarchical 8-PSK were not obtained within a specified time limited by a maximum number of iterations. As such the symbol was transmitted from a uniform 8-PSK. Table 3.3 shows the sample average gains with the proposed scheme for different average CNR $(\bar{\gamma})$. For a given average CNR $\bar{\gamma}$, 1000 combinations of CNRs (i.e., γ_1, γ_2 and γ_3) were generated according to an

Table 3.1. *Gain over adaptive uniform PSK with TDM and the obtained angles for multimedia transmission.*

Service Class	QoS parameters		θ_1 (rad)	θ_2 (rad)	Gain (dB)
	avg. BER	Rate			
S_3	10^{-4}	$2R_b$	0.7644	0.3052	0.6880
S_1	10^{-2}	R_b			
S_4	10^{-5}	$2R_b$	0.7684	0.2770	0.9497
S_1	10^{-2}	R_b			
S_5	10^{-6}	$2R_b$	0.7711	0.2560	1.1369
S_1	10^{-2}	R_b			
S_3	10^{-4}	$2R_b$	0.7673	0.3625	0.2022
S_2	10^{-3}	R_b			
S_5	10^{-5}	$2R_b$	0.76	0.3327	0.4507
S_2	10^{-3}	R_b			
S_6	10^{-6}	$2R_b$	0.7728	0.3098	0.6394
S_2	10^{-3}	R_b			

exponential distribution. The number of times ($\mathcal{N}$) in which the optimum transmission parameters with hierarchical 8-PSK are found is also shown in Table 3.3. Note that $\mathcal{N}$ depends on the average CNR. For instance, at high average CNR, $\mathcal{N}$ is low but the gain is almost 1 dB. Though the Monte-Carlo simulation does not converge due to the generation of correlated samples, sample averages show that the proposed scheme is more energy efficient than the adaptive uniform PSK in TDM. For a given combination of link qualities, the gain depends on the required BER of the multicasted message. For the combination of $\gamma_1 = -5$ dB, $\gamma_2 = 10$ dB and $\gamma_3 = 15$ dB as shown in example 10 in Table 3.2, the gains are 2.06 dB, 2.28 dB and 2.55 dB for BER of 10^{-3}, 10^{-4} and 10^{-5}, respectively.

Table 3.2. *Gain over adaptive uniform PSK with TDM for multicasting with a data rate of R_b and BER of 10^{-3}.*

Example #	γ_1 (dB)	γ_2 (dB)	γ_3 (dB)	Gain (dB)
1	-5	0	0	0.75
2	-5	0	5	1.82
3	-5	0	10	2.57
4	-5	0	15	2.96
5	-5	0	20	3.13
6	-5	5	10	2.66
7	-5	5	15	1.64
8	-5	5	20	3.12
9	-5	10	10	2.80
10	-5	10	15	2.06
11	-5	10	20	0.00
12	-5	15	15	3.14
13	-5	15	20	2.25
14	5	5	5	0.00

Table 3.3. *Sample average gain of* 1000 *randomly generated cases at different average CNR* ($\bar{\gamma}$) *for multicasting (data rate=*R_b *and BER=*10^{-3}*).*

$\bar{\gamma}$ (dB)	Gain (dB)	$\mathcal{N}$
-3	1.0234	893
-2	0.7129	890
-1	0.9624	915
0	0.5547	913
1	0.8023	912
2	0.4820	918
3	0.5958	911
4	0.7379	907
5	0.9320	899
6	1.1001	912
7	0.8346	914
8	0.5926	908
9	0.9026	909
10	0.9522	913
11	1.0754	921
12	0.7560	921
13	0.9125	910
14	1.1286	900
16	0.5630	764
18	1.2226	540
20	1.0828	326

Note: $\mathcal{N}$ is the number of times in which optimum parameters with hierarchical 2/4/8-PSK were found in 1000 simulation runs.

Chapter 4

Simultaneous Voice and Multi-Class Data Transmission

Considerable research efforts have focused on the development of a variety of MAC techniques and protocols such as PMRA, I-ISMA, and D-TDMA for the integration of voice and data for wireless communication system. Some of the references are mentioned in Chapter 1. Recently, Alouini *et al.* and Hwang *et al.* proposed link layer solution to the voice and single class of data integration problem in [17] and [18], respectively.

The scheme proposed in [17] uses hybrid BPSK/M-AM modulation scheme to transmit voice and data in the same message string. It devotes the quadrature (Q) channel to voice transmission with variable power BPSK while transmitting data over the inphase (I) channel with variable-rate M-AM. To take advantage of the time-varying nature of fading, it dynamically allocates power between the I and Q channels. The power allocated to the Q channel is just to meet the target BER for voice, BER_v, and the remaining power is allocated to the I channel to support data with M-AM below the data target BER, BER_d. Since M-AM is spectrally less efficient than the M-QAM, an adaptive technique employing variable rate uniform M-QAM was proposed in [18]. It also changes the constellation size dynamically to take advantage of the time-varying nature of fading. To meet the satisfactory communication, one sub-channel (meaning a bit position in a symbol) is proposed to devote for voice communication while other available sub-channels are used to transmit data. However, due to the use of uniform M-QAM constellation, the alphabet size is se-

lected so that, on the average, both the voice and data are transmitted below the target data BER, BER_d. Therefore, the voice bit gets unnecessary extra protection at the expense of spectral efficiency (at low CNR) and outage probability for data transmission.

In this chapter, we propose a new adaptive hierarchical technique as a link layer solution to the voice and different classes of data integration problem. More generally, the proposed scheme is capable of handling three independent information streams which may differ in their delay and BER requirements and can easily be extended for more than three different classes of data transmission. To take advantage of the time-varying nature of the channel, the scheme adapts not only the alphabet size but also the priority parameters of hierarchical signal constellation which control the relative BERs of different position bits. The newly proposed adaptive scheme devotes only one sub-channel for voice bit to meet the stringent delay requirement of voice communication while devoting all other sub-channels to variable-rate data transmission. As we will see latter in this chapter, the new scheme offers a higher spectral efficiency for data transmission than the schemes employing hybrid BPSK/M-AM and uniform M-QAM.

The organization of this chapter is as follows. Section 4.1.1 describes the proposed hierarchical scheme for voice and two different classes of data transmission. To compare the proposed scheme with the schemes employing hybrid BPSK/M-AM and uniform M-QAM, we have extended the proposed schemes in [17] and [18] for voice and two different classes of data transmission in Section 4.1.2. Assuming perfect channel estimation and negligible time delay, the performances of the new scheme and the extended schemes are analyzed in Section 4.2.1. In particular, closed-form expressions for the outage probability, the achievable spectral efficiency and average BER for voice and data (both classes) transmission are derived. Numerical results that allow us to compare the behaviors of the different schemes under consideration are also presented in this Section. Finally, Section 4.2.2 shows the performance of voice and single class data transmission using hierarchical M-QAM which is a special case of voice and two different classes of data transmission.

4.1 Voice and Two Classes of Data Transmission

4.1.1 Proposed Adaptive Hierarchical Scheme

The block diagram of the proposed scheme is shown in Fig. 4.1. Assuming a perfect channel fading amplitude estimate, $\hat{\alpha} = \alpha$ (equivalently, a perfect channel CNR estimation, $\hat{\gamma} = \gamma$), and a fixed transmit power, $P(\gamma)$[W], same as a peak power constraint, P[W], we now describe the details of our proposed system. According to the CNR estimate, the transmission parameters of constant power hierarchical M-QAM constellation are selected to support the voice as well as Class-I and/or Class-II data below their respective target BERs. Without loss of generality, we assume that the required BER of voice, Class-I and Class-II data, are BER_v, BER_{d1}, and BER_{d2}, respectively where $\text{BER}_v > \text{BER}_{d1} > \text{BER}_{d2}$. Since voice signal requires the least protection and a continuous fixed-rate transmission, the LSB position sub-channel of the Q channel of a variable size hierarchical QAM constellation is devoted for the voice communication. The remaining $(\log_2 M - 1)$ data sub-channels are assigned to two different classes of data according to the selected priority parameters. If the channel condition is not good enough to support one bit voice and one bit Class-I data with the hierarchical 4-QAM below the target voice BER BER_v and Class-I data BER BER_{d1}, it only transmits voice using BPSK modulation. Hence, based on the channel CNR estimate, the decision device at the receiver selects the transmission parameters to be transmitted, assigns available data sub-channels to two classes of data, configures the demodulator accordingly, and informs the transmitter about that decision via the feedback path. We now describe the constellation size and parameter selection as well as sub-channel assignment to different classes of data in more details. To minimize the average power consumption subject to the peak power constraint, the proposed scheme does not attempt to transmit when the channel condition is not good enough to support satisfactory voice communication i.e., the estimated CNR is less than γ_0 where γ_0 is obtained from the exact BER of

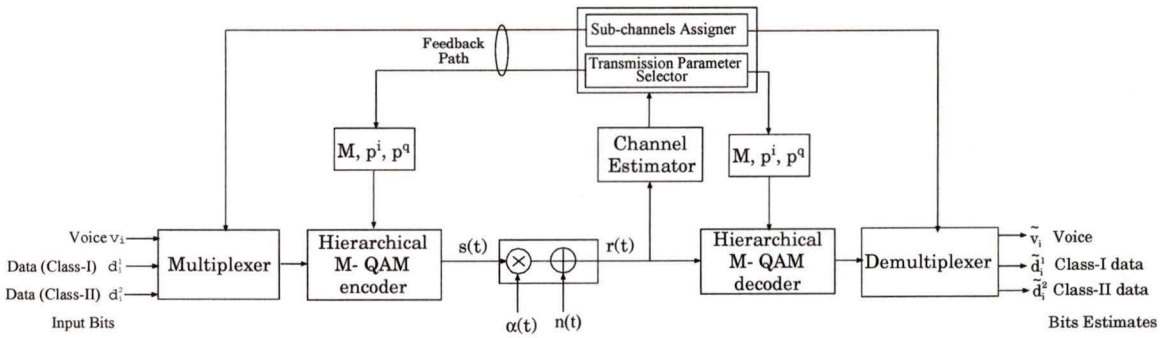

Figure 4.1. *Block diagram of the proposed adaptive technique.*

BPSK over AWGN channel modulation given by

$$\text{BER}_{BPSK} = \frac{1}{2}\text{erfc}(\sqrt{\gamma}) \tag{4.1}$$

where erfc $(\cdot)$ denotes the complementary error function. To transmit data, the scheme varies its constellation size M and priority vectors $\mathbf{p}^i$ and $\mathbf{p}^q$ according to the instantaneous channel CNR fluctuation as follows. The CNR range, in which any kind of data is transmitted is divided into R fading regions and each fading region is assigned a unique constellation size. Specifically, the constellation size $M_r = 2^{r+1}$ (where r is the total number of data bits per hierarchical M_r-QAM symbol) is assigned to the r-th fading region $(r = 1, 2, \cdots, R)$. When the received data CNR is estimated to be in the r-th fading region, the constellation size M_r is transmitted. The region boundaries (or constellation size switching thresholds) $\{\gamma_r\}_{r=1}^{R+1}$ are set to the CNR such as the voice bit in the LSB position of the Q channel and Class-I data bits assigned to the remaining r sub-channels, are sent below their respective target BERs over AWGN channel using hierarchical M_r-QAM constellation. Since the BER expressions for hierarchical M-QAM in (2.18)-(2.21) are not invertible, the region boundaries γ_r $(r = 1, 2, \cdots, R+1)$ are obtained by numerically optimizing the $(r+1)$ BER equations of hierarchical M_r-QAM over AWGN channel for the priority parameters ($\mathbf{p}^i$ and $\mathbf{p}^q$) and the CNR γ and setting $\gamma_{R+1} = +\infty$.

From (2.18) to (2.21), it is evident that for a given size of hierarchical QAM constellation, BER performances of different position bits in a transmitted symbol depend on the

CNR γ as well as the priority vectors $\mathbf{p}^i$ and $\mathbf{p}^q$. Therefore, for a given alphabet size i.e., in a given fading region, the choice of available data sub-channels assignment to different classes of data i.e., the number as well as the positions of the sub-channels that can be assigned to each class of data depends on the priority parameters and the received CNR. To select the parameters and assign available sub-channels to different classes of data accordingly, each of the R fading regions is divided into a number of fading sub-regions and each sub-region is assigned a set of optimized priority vectors to support a unique combination of data bits from two different classes of data. Specifically, r-th fading region is divided into $(r+1)$ sub-regions and when the CNR is estimated in the s-th sub-region $(s = 1, 2, \cdots, r+1)$, parameters, $\mathbf{p}^i_{rs}$ and $\mathbf{p}^q_{rs}$ are transmitted. These vectors, $\mathbf{p}^i_{rs}$ and $\mathbf{p}^q_{rs}$ are selected so that the voice in the LSB position sub-channel of the Q channel, Class-II data bits assigned to $(s-1)$ data sub-channels of higher significance and Class-I data bits in the remaining $(r-s+1)$ data sub-channels are transmitted below their respective target BERs. For example, the details of data sub-channels assignment to different classes of data in different sub-regions for a maximum constellation size of 6 (i.e., 64-QAM) are shown in Table 4.1. From the Table, it is evident that if the CNR improves from one sub-region to the next, in a given region, one bit of Class-I data from higher significance bit position sub-channel is replaced by a Class-II data bit. Specifically, in the first sub-region of r-th region, all the r data sub-channels are assigned to Class-I data service. In the next sub-region, $(r-1)$ data sub-channels of higher significance are assigned to class-I while assigning one data sub-channel to Class-II data and so on until all the r data sub-channels are assigned to data Class-II in $(r+1)$-th sub-region. The sub-region boundaries $\{\gamma^s_r\}^{R,r+1}_{r=1,s=1}$ as well as the priority parameters, $\{\mathbf{p}^i_{rs}\}^{R,r+1}_{r=1,s=1}$ and $\{\mathbf{p}^q_{rs}\}^{R,r+1}_{r=1,s=1}$ are obtained by numerically optimizing the BER equations of hierarchical M_r-QAM such as the assigned data (Class-I and/or Class-II) and voice bits, according to the Table 4.1, are sent below their respective target BERs over AWGN channel. For example, the sub-region boundary γ^2_3 and priority parameters for the 2nd sub-region of the 3rd fading region are obtained by numerically

optimizing (2.18) and (2.19) for the transmission parameters such as

$$\begin{aligned} P_b^s(M_3, \gamma_3^2, \mathbf{p}_{32}^i, \mathbf{p}_{32}^q, i_1) &\leq \text{BER}_{d_1} \\ P_b^s(M_3, \gamma_3^2, \mathbf{p}_{32}^i, \mathbf{p}_{32}^q, i_2) &\leq \text{BER}_{d_1} \\ P_b^s(M_3, \gamma_3^2, \mathbf{p}_{32}^i, \mathbf{p}_{32}^q, q_1) &\leq \text{BER}_{d_2} \\ P_b^s(M_3, \gamma_3^2, \mathbf{p}_{32}^i, \mathbf{p}_{32}^q, q_2) &\leq \text{BER}_v \end{aligned}$$

where $\mathbf{p}_{32}^i$ and $\mathbf{p}_{32}^q$ represent the optimized quadrature and inphase channel priority vector, respectively, in 2nd sub-region of 3rd fading region. It is important to note that the first sub-region boundaries $\{\gamma_r^1\}_{r=1}^{R+1}$ are equal to their corresponding region boundaries $\{\gamma_r\}_{r=1}^{R+1}$.

According to the proposed sub-channel assignment scheme, all the R data sub-channels are assigned to Class-II data if the CNR estimate falls anywhere between the γ_R^{R+1} and $+\infty$. Therefore, the Class-I data throughput, in this CNR range, becomes zero. To transmit both classes of data with equal importance, fifty percent of the time Class-II data is transmitted while for the remaining fifty percent of the time Class-I data is transmitted in this range. As an example, the instantaneous spectral efficiency according to the proposed scheme are illustrated in Fig. 4.2 for a maximum constellation size of 6. The switching thresholds γ_r^s are shown symbolically (not numerical values) to explain the shape of the curve. When the instantaneous CNR is less than γ_0, transmission is not attempted while only one bit voice is transmitted in the range between γ_0 and γ_1. Above γ_1, both voice and data (Class-I and/or Class-II) are transmitted simultaneously. In a given CNR range, the instantaneous data efficiencies are staircase like curves as one bit of Class-I data is replaced by one bit of Class-II when the CNR improves from one sub-region to the next. In the range of CNR from γ_5^6 to $+\infty$, both classes of data have the same spectral efficiency as they are sent alternately in this range.

4.1.2 Comparison with Hybrid BPSK/M-AM and Uniform M-QAM

In an attempt to transmit integrated voice/data traffic over fading channels, the adaptive hybrid BPSK/M-AM and uniform M-QAM were used in [17] and [18], respectively. Both

Table 4.1. *Sub-channel assignments for voice (v), Class-I data (d_1) and Class-II data (d_2).*

Fading region, r	Sub-regions, s	Sub-channel assignments
1	1	I-d_1, Q-v
	2	I-d_2, Q-v
2	1	I-d_1, Q-d_1v
	2	I-d_1, Q-d_2v
	3	I-d_2, Q-d_2v
3	1	I-d_1d_1, Q-d_1v
	2	I-d_1d_1, Q-d_2v
	3	I-d_2d_1, Q-d_2v
	4	I-d_2d_2, Q-d_2v
4	1	I-d_1d_1, Q-d_1d_1v
	2	I-d_1d_1, Q-d_2d_1v
	3	I-d_2d_1, Q-d_2d_1v
	4	I-d_2d_1, Q-d_2d_2v
	5	I-d_2d_2, Q-d_2d_2v
5	1	I-$d_1d_1d_1$, Q-d_1d_1v
	2	I-$d_1d_1d_1$, Q-d_2d_1v
	3	I-$d_2d_1d_1$, Q-d_2d_1v
	4	I-$d_2d_1d_1$, Q-d_2d_2v
	5	I-$d_2d_2d_1$, Q-d_2d_2v
	6	I-$d_2d_2d_2$, Q-d_2d_2v

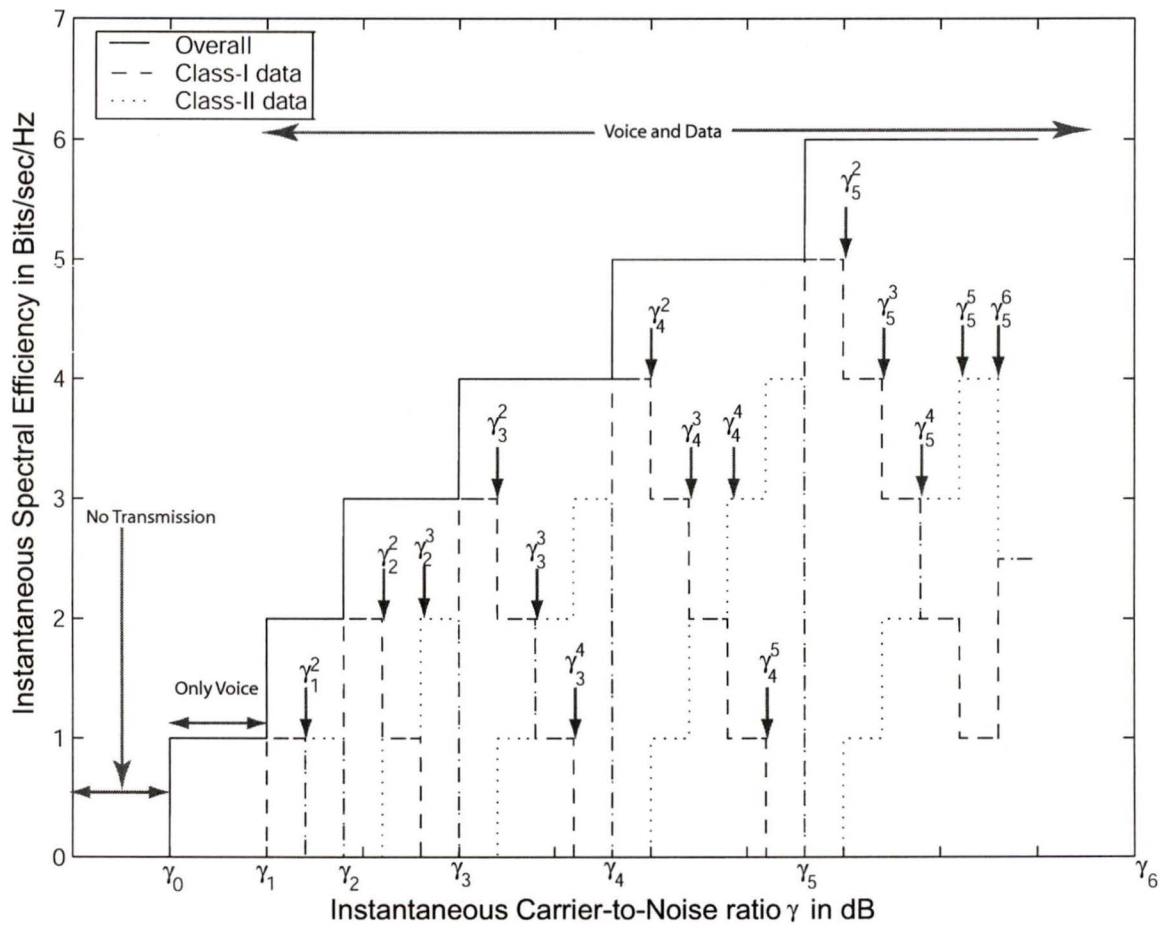

Figure 4.2. *Instantaneous spectral efficiency versus instantaneous CNR γ.*

schemes were proposed to transmit voice as well as single class of data. However, they can be extended to transmit voice as well as two different classes of data requiring two different BERs as follows.

4.1.2.1 Hybrid BPSK/M-AM

For hybrid BPSK/M-AM, the basic transmission scheme (i.e., voice over the Q channel with variable power BPSK and data over the I channel with variable rate M-AM) and the power allocation scheme (i.e., the power allocated to the I channel, $P_v(\gamma)$ to just meet the voice target BER, BER_v while the remaining available power $P_d(\gamma) = P - P_v(\gamma)$ is allocated to the Q channel to support data with M-AM) still remain the same as was proposed and described in [17]. The size of AM constellation, $M_r^{(\text{AM})} = 2^r$ (where r is the number of data bits per $M_r^{(\text{AM})}$-AM symbol) is selected by dividing the data CNR $\gamma_d = \alpha^2 P_d / N_0 W$ range into $(R+1)$ fading regions [17]. The region boundaries (i.e., switching thresholds), $\{\gamma_{d_r}\}_{r=1}^{R+1}$ are set to the CNR required to achieve the target Class-I data BER, BER_{d_1} using $M_r^{(\text{AM})}$-AM over an AWGN channel. Specifically from [17, Eq. (12)] we have

$$\begin{aligned} \gamma_{d_r} &= \frac{1-2^{2r}}{3}\ln(10\text{BER}_{d_1}); \quad r = 0, 1, 2, \cdots, R, \\ \gamma_{d_{R+1}} &= +\infty. \end{aligned} \tag{4.2}$$

To reduce average power consumption, the transmitter does not attempt to transmit voice if the satisfactory voice communication is not possible by allocationg all the power P[W] to Q channel for voice communication i.e., the voice CNR $\gamma_v = \alpha^2 P_v / N_0 W$ is than γ_{v_1} where $\gamma_{v_1} = \gamma_0$. In this case a voice outage is declared [17].

To transmit two classes of data, each of the $R+1$ fading regions is divided into two sub-regions and each sub-region is assigned a unique class of data bit. Specifically, if the CNR estimate falls in the first sub-region of r-th fading region ($r = 0, 1, \cdots, R$), all the r data bits are sent from the Class-I data while, in the second sub-region, all the r data bits are sent from the Class-II data. In a given fading region r, the first sub-region boundary, $\gamma_{d_r}^1$ is identical to the corresponding region boundary γ_{d_r} and the second sub-region boundary $\gamma_{d_r}^2$

are set to the CNR required to achieve the target BER_{d_2} using $M_r^{(\text{AM})}$-AM over an AWGN channel. Specifically from [17, Eq. (12)], we have

$$\gamma_{d_r}^2 = \frac{1-2^{2r}}{3}\ln(10\text{BER}_{d_2}); \quad r = 0, 1, \cdots, R. \tag{4.3}$$

According to the proposed data assignment scheme, the Class-I data throughput reduces to zero if the data CNR falls anywhere between γ_R^2 and $+\infty$. So, rather than transmitting all the time Class-II data in this region, fifty percent of the time Class-I data is transmitted and for the remaining fifty percent of the time Class-II data is transmitted.

4.1.2.2 Uniform M-QAM

Uniform M-QAM was used in [18] for simultaneous voice and single class data transmission. In this case, for bad channel conditions, BPSK is used only to transmit voice below target voice BER, BER_v while using uniform M_r-QAM ($M_r = 2^{r+1}$) constellation for favorable channel conditions to transmit one bit voice and r bits data below data target BER BER_d. To select the alphabet size M_r, the CNR range is divided into number of regions. More specifically, the CNR range is divided in to $R+1$ fading regions and $M_r = 2^{r+1}$ uniform QAM constellation is transmitted if the CNR falls in region r ($r = 0, 1, 2 \cdots, R$). The switching thresholds $\{\gamma_r\}_{r=1}^R$ are obtained using [18, Eq. (5)]

$$\begin{aligned} \gamma_r &= \frac{1-2^{r+1}}{1.5}\ln(5\text{BER}_{d_1}); \quad r = 1, 2, \cdots, R, \\ \gamma_{R+1} &= +\infty. \end{aligned} \tag{4.4}$$

The scheme can also be extended to transmit voice as well as two different classes of data by dividing each data CNR region into two sub-regions and transmitting Class-I data in the first sub-region and Class-II data in the second sub-region as described above for BPSK/M-AM. The first sub-region boundaries $\{\gamma_r^1\}_{r=1}^R$ are identical to region boundaries $\{\gamma_r\}_{r=1}^R$ and the second sub-region boundaries are obtained using [18, Eq. (5)]

$$\gamma_r^2 = \frac{1-2^{r+1}}{1.5}\ln(5\text{BER}_{d_2}); \quad r = 1, 2, \cdots, R. \tag{4.5}$$

To reduce average power consumption, similarly the transmitter does not attempt to transmit if the CNR estimate is less than γ_0 and in this case a voice outage is declared.

It is important to mention that both the extended schemes transmit at most two different kind of bits (voice and Class-I or Class-II data) in each symbol whereas the adaptive hierarchical schemes can transmit three different bits (voice, Class-I data and Class-II data) in each symbol.

4.2 Performance

In this section, we analyze the performance of our new proposed scheme for voice and two different classes of data transmission. This analysis also evaluates as a byproduct the performance of voice and single class data transmission which has been compared to the schemes proposed in [17] and [18]. The numerical results, for different values of the Nakagami fading parameters m, are plotted in Figs.4.3 -4.12. In our numerical results, we assume a target uncoded voice BER, BER_v, of 10^{-2}, a target uncoded Class-I data BER, BER_{d_1}, of 10^{-4}, and a target uncoded Class-II data BER, BER_{d_2}, of 10^{-6}.

We use the MATLAB Optimization and Statistics Toolbox to obtain the numerical results. We assume perfect channel estimation, coherent phase detection at the receiver, and Gray coding for bit mapping on the signal constellations, as shown in Fig. 2.2. In the examples, we use maximum constellation size 64 for both hierarchical QAM and uniform QAM and 32-AM for hybrid BPSK/M-AM modulations.

4.2.1 Voice and Two Classes of Data Transmission

4.2.1.1 Outage Probability

Since voice transmission is not attempted when the CNR drops below γ_0, the voice outage probability, P_{out}^v is given as [17]

$$P_{\text{out}}^v = \int_0^{\gamma_0} p_\gamma(\gamma) d\gamma \tag{4.6}$$

Using (2.3), we get

$$\begin{aligned} P_{\text{out}}^{v} &= \int_{0}^{\gamma_0} \left(\frac{m}{\bar{\gamma}}\right)^{m} \frac{\gamma^{m-1}}{\Gamma(m)} \exp\left(-m\frac{\gamma}{\bar{\gamma}}\right) d\gamma \\ &= 1 - \frac{\Gamma\left(m, m\frac{\gamma_0}{\gamma}\right)}{\Gamma(m)} \end{aligned} \tag{4.7}$$

where $\Gamma(\cdot,\cdot)$ is the complementary incomplete gamma function (or Prym's function) defined by [26, p. 949, Eq. (8.350.2)]

$$\Gamma(z,\mu) = \int_{\mu}^{+\infty} t^{z-1}e^{-t}dt. \tag{4.8}$$

The voice outage probabilities for the extended schemes with hybrid BPSK/M-AM and uniform M-QAM are identical to (4.7) as they do not send voice if the CNR is less than γ_0. The voice outage probability for different values of Nakagami fading parameter m is shown in Fig. 4.3. All the scheme has the same voice outage as all of them send voice using BPSK when the channel CNR is good enough to support BPSK with voice target BER. From the figure, it is evident that the outage probability decreases as m increase. This is due to the fact that as m increases the amount of multipath fading on the channel decreases as discussed in Chapter 1.

Since Class-I data and Class-II data are not sent when the CNR estimate is lower than γ_1^1 and γ_1^2, respectively, the outage probabilities of Class-I data $P_{\text{out}}^{d_1}$ and Class-II data $P_{\text{out}}^{d_2}$ are given as

$$P_{\text{out}}^{d_1} = \int_{0}^{\gamma_1^1} p_\gamma(\gamma)d\gamma = 1 - \frac{\Gamma\left(m, m\frac{\gamma_1^1}{\bar{\gamma}}\right)}{\Gamma(m)}, \tag{4.9}$$

$$P_{\text{out}}^{d_2} = \int_{0}^{\gamma_1^2} p_\gamma(\gamma)d\gamma = 1 - \frac{\Gamma\left(m, m\frac{\gamma_1^2}{\bar{\gamma}}\right)}{\Gamma(m)}. \tag{4.10}$$

Similarly, the outage probabilities for data with hybrid BPSK/M-AM are given by

$$P_{\text{out}}^{d_1} = 1 - \frac{\Gamma\left(m, m\frac{\gamma_{v_1}+\gamma_{d_1}^1}{\bar{\gamma}}\right)}{\Gamma(m)}, \tag{4.11}$$

$$P_{\text{out}}^{d_2} = 1 - \frac{\Gamma\left(m, m\frac{\gamma_{v_1}+\gamma_{d_1}^2}{\bar{\gamma}}\right)}{\Gamma(m)}, \tag{4.12}$$

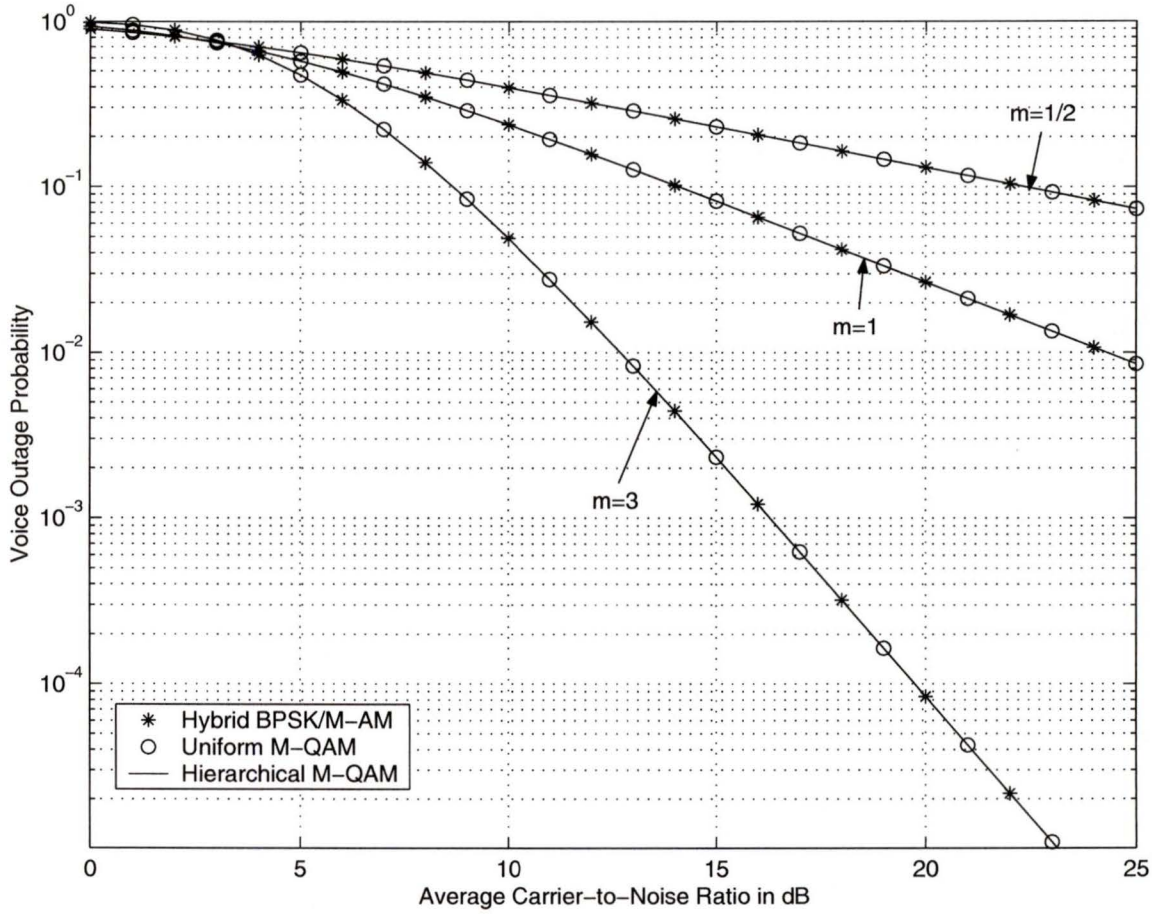

Figure 4.3. *Outage probability for voice transmission versus the average CNR* $\bar{\gamma}$.

where γ_{v_1}, $\gamma_{d_1}^2$ and $\gamma_{d_1}^1$ are the first voice , Class-II and Class-I data switching thresholds, respectively with hybrid BPSK/M-AM. The outage probabilities for data transmission with the uniform M-QAM can be obtained from (4.9) and (4.10) using the first data switching thresholds γ_1^1 (for Class-I) and γ_1^2 (for Class-II) of the extended scheme with uniform M-QAM.

For three different schemes, the outage probabilities for Class-I and Class-II data transmission are plotted in Fig. 4.4 and Fig. 4.5, respectively for different values of Nakagami fading parameters m. These figure show that the proposed scheme has the same data outage probability as with hybrid BPSK/M-AM but lower than that with uniform M-QAM. This is expected as the hybrid BPSK/2-AM and hierarchical 4-QAM are equivalent to each other and they require same CNR to send one bit voice and one bit data below their respective target BERs. With uniform 4-QAM, both the voice and data are sent below the data target BER which in turn requires higher CNR and causes higher data outage probability. For example, both the BPSK/2-AM and the hierarchical 4-QAM require 9.8325 dB CNR to transmit one bit voice with a BER of 10^{-2} and one bit of data with a BER of 10^{-4} while the uniform 4-QAM requires 11.8 dB CNR to transmit two (one bit voice and one bit Class-I data) bits with a average BER of 10^{-4}.

4.2.1.2 Achievable Spectral Efficiency

The average link spectral efficiency for voice transmission $\langle R_v \rangle / W$ is given by [17]

$$\frac{\langle R_v \rangle}{W} = 1 - P_{\text{out}}^v = \frac{\Gamma\left(m, m\frac{\gamma_0}{\bar{\gamma}}\right)}{\Gamma(m)} \tag{4.13}$$

The average link spectral efficiency for voice transmission with extended schemes employing BPSK/M-AM and uniform M-QAM is identical to 4.13, respectively. Since all the schemes start to transmit voice when the channel is good enough to support voice using BPSK below voice target BER, BER_v, they provide same spectral efficiency for voice transmission as shown in Fig. 4.10 and Fig. 4.11 for two different values of Nakagami fading parameter m.

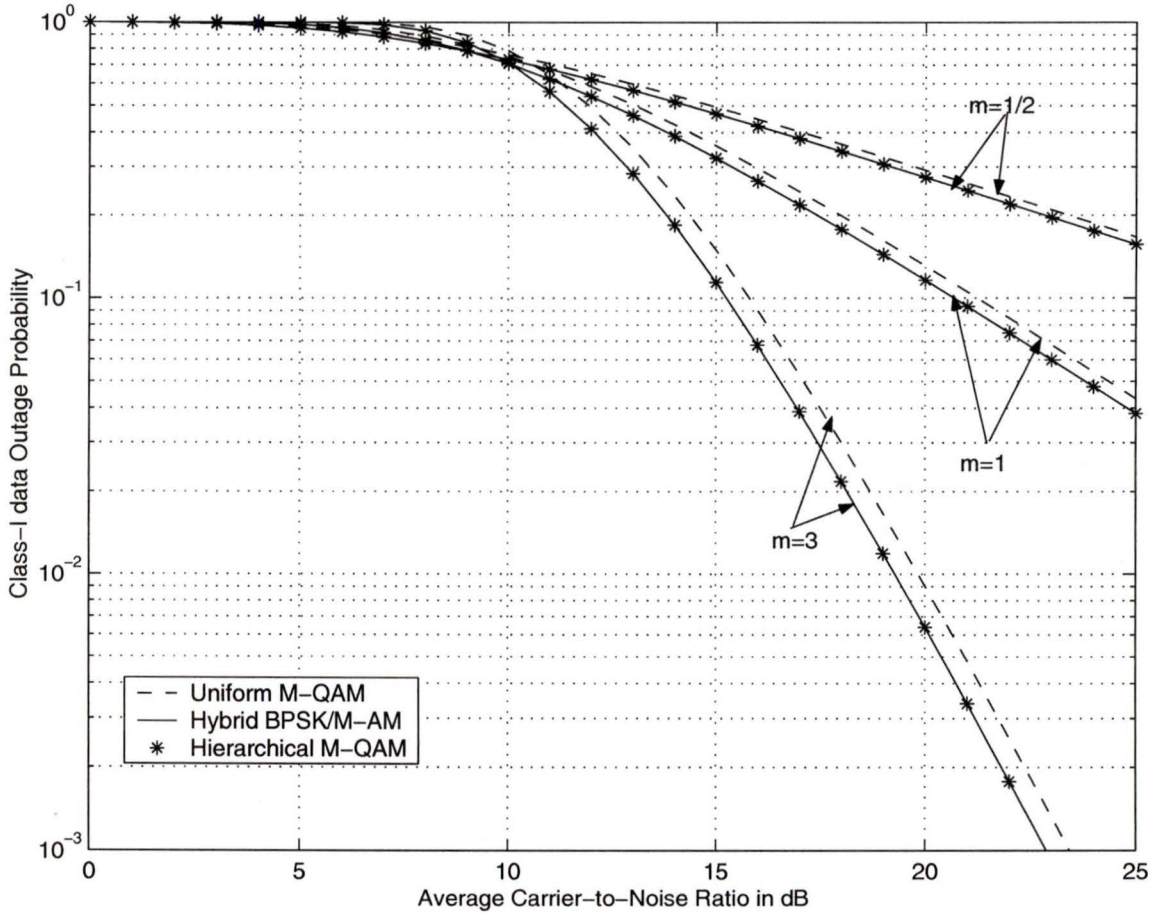

Figure 4.4. *Class-I data outage probability versus the average CNR* $\bar{\gamma}$.

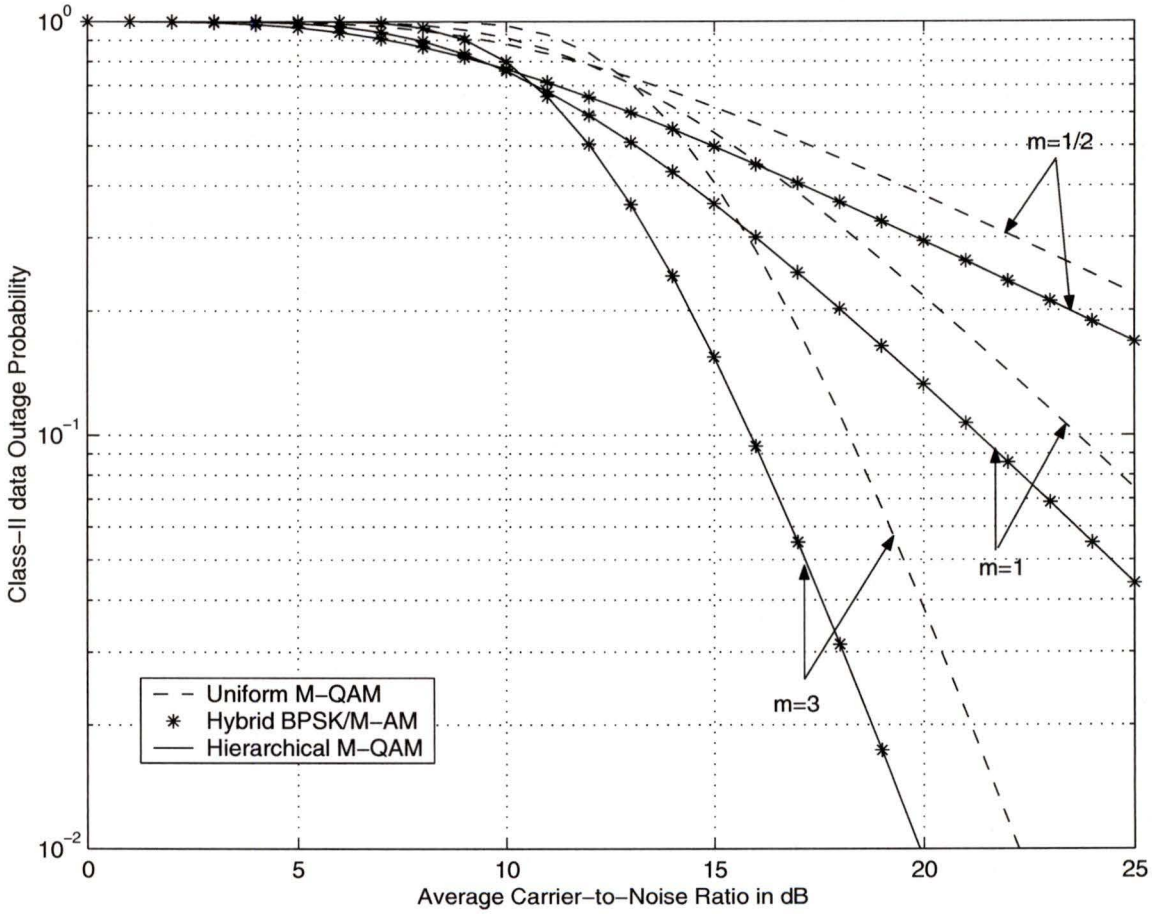

Figure 4.5. *Class-II data outage probability versus the average CNR* $\bar{\gamma}$.

The average link spectral efficiency for data transmission $\langle R_{d_i} \rangle / W$ $(i = 1, 2)$ are just the sum of data rates associated with the individual sub-regions of each region, weighted by the probability

$$a_{rs} = \begin{cases} \int_{\gamma_r^s}^{\gamma_r^{s+1}} p_\gamma(\gamma) d\gamma & \text{for } s = 1, 2, \cdots, r \\ \\ \int_{\gamma_r^s}^{\gamma_s^1} p_\gamma(\gamma) d\gamma & \text{for } s = r+1 \end{cases} \tag{4.14}$$

that the CNR γ falls in s-th sub-region in the r-th fading region

$$\frac{\langle R_{d_1} \rangle}{W} = \sum_{r=1}^{R} \sum_{s=1}^{r+1} (r - s + 1) a_{rs} + \frac{1}{2} R \, a_{RR+1} \tag{4.15}$$

$$\frac{\langle R_{d_2} \rangle}{W} = \sum_{r=1}^{R} \sum_{\substack{s=1 \\ s \neq R+1}}^{r+1} (s - 1) a_{rs} + \frac{1}{2} R \, a_{RR+1} \tag{4.16}$$

where the a_{rs}'s can be expressed as

$$a_{rs} = \begin{cases} \frac{\Gamma\left(m, m\frac{\gamma_r^s}{\bar{\gamma}}\right) - \Gamma\left(m, m\frac{\gamma_r^{s+1}}{\bar{\gamma}}\right)}{\Gamma(m)} & \text{for } s = 1, 2, \cdots, r \\ \frac{\Gamma\left(m, m\frac{\gamma_r^s}{\bar{\gamma}}\right) - \Gamma\left(m, m\frac{\gamma_s^1}{\bar{\gamma}}\right)}{\Gamma(m)} & \text{for } s = r+1. \end{cases} \tag{4.17}$$

The extended scheme with hybrid BPSK/M-AM leads to the following data spectral efficiency equations

$$\frac{\langle R_{d_1} \rangle}{W} = \sum_{r=1}^{R} r b_r^1 + \frac{1}{2} R \, b_R^2 \tag{4.18}$$

$$\frac{\langle R_{d_2} \rangle}{W} = \sum_{r=1}^{R-1} r b_r^2 + \frac{1}{2} R \, b_R^2 \tag{4.19}$$

where b_r^1's and b_r^2's are the probabilities that the data CNR γ_d falls in the first and second sub-region of the r-th fading region, respectively and given by

$$b_r^1 = \frac{\Gamma\left(m, m\frac{\gamma_{v_1} + \gamma_{d_r}^1}{\bar{\gamma}}\right) - \Gamma\left(m, m\frac{\gamma_{v_1} + \gamma_{d_r}^2}{\bar{\gamma}}\right)}{\Gamma(m)} \tag{4.20}$$

$$b_r^2 = \frac{\Gamma\left(m, m\frac{\gamma_{v_1} + \gamma_{d_r}^2}{\bar{\gamma}}\right) - \Gamma\left(m, m\frac{\gamma_{v_1} + \gamma_{d_{r+1}}^1}{\bar{\gamma}}\right)}{\Gamma(m)}. \tag{4.21}$$

where $\{\gamma_{d_r}^1\}_{r=1}^R$ and $\{\gamma_{d_r}^2\}_{r=1}^R$ are the first and second sub-region boundaries respectively for the scheme employing BPSK/M-AM.

The expressions of achievable spectral efficiencies for data transmission with the extended scheme employing uniform M-QAM are same as (4.18) and (4.19) where the probabilities b_r^1's and b_r^2's are calculated using the sub-region boundaries of the extended scheme employing uniform M-QAM. Specifically, the probabilities are expressed as

$$b_r^1 = \frac{\Gamma\left(m, m\frac{\gamma_r^1}{\bar{\gamma}}\right) - \Gamma\left(m, m\frac{\gamma_r^2}{\bar{\gamma}}\right)}{\Gamma(m)} \tag{4.22}$$

$$b_r^2 = \frac{\Gamma\left(m, m\frac{\gamma_r^2}{\bar{\gamma}}\right) - \Gamma\left(m, m\frac{\gamma_{r+1}^1}{\bar{\gamma}}\right)}{\Gamma(m)} \tag{4.23}$$

where $\{\gamma_r^1\}_{r=1}^R$ and $\{\gamma_r^2\}_{r=1}^R$ are the first and second sub-region boundaries respectively for the scheme employing uniform M-QAM. The achievable spectral efficiencies for both classes of data transmission are plotted in Figs. 4.6-4.7 for different values of the Nakagami fading parameter m. From these figures, it is evident that the proposed new scheme always offers higher spectral efficiency for both classes of data transmission than the extended scheme employing hybrid BPSK/M-AM except slightly lower efficiency for Class-I data transmission at very low CNR range. On the other hand, the scheme employing uniform M-QAM offers higher spectral efficiency for Class-I data transmission than the new scheme at the expense of very low spectral efficiency for Class-II data transmission. This occurs due to the fact that the choice of sub-channel assignment and switching thresholds with all these schemes are done in a conservative fashion. For example, with hierarchical QAM constellations, as soon as the estimated CNR supports a new bit from service Class-II, it attempts to transmit the new bit replacing one bit of Class-I data which is obvious from Table 4.1. Similarly, in a given fading region, the extended schemes attempt to transmit bits from service Class-II as soon as the the estimate CNR is good enough to support the data below the target BER, BER_{d_2}. Therefore, there is no mechanism to control the relative data throughput of Class-I and Class-II data. However, due to the capability of

handling three kind of bits in the same message symbol, the adaptive hierarchical scheme achieves better data throughput fairness (for both classes of data) compared to the extended schemes which offer higher throughput for one class of data at the expense of other as clearly shown in Figs.4.6-4.7. After all, the new scheme always offers higher overall data spectral efficiency than both the extended schemes as shown in Fig. 4.8.

4.2.1.3 Average BER

Since the choice of the constellation size and the priority vectors are done in a conservative fashion with hierarchical constellation, both voice and data (Class-I and Class-II) are transmitted at their average BERs smaller than their respective target BERs. Let us consider voice, Class-I data and Class-II data are transmitted at average BER, $\langle \text{BER}_v \rangle$, $\langle \text{BER}_{d_1} \rangle$ and $\langle \text{BER}_{d_2} \rangle$, respectively. Theses average BERs can be computed as the ratio of the average number of bits in error over the total average number of transmitted bits yielding

$$\langle \text{BER}_v \rangle = \frac{\overline{\text{BER}}_{BPSK} + \sum_{r=1}^{R} \sum_{s=1}^{r+1} \sum_{i_{rs}^v} \overline{\text{BER}}_{rs}(i_{rs}^v)}{\langle R_v/W \rangle}, \tag{4.24}$$

$$\langle \text{BER}_{d_1} \rangle = \frac{\sum_{r=1}^{R} \sum_{s=1}^{r+1} \sum_{i_{rs}^1} \overline{\text{BER}}_{rs}(i_{rs}^1) + \frac{1}{2} \sum_{i_{RR+1}^1} \overline{\text{BER}}_{RR+1}(i_{RR+1}^1)}{\langle R_{d_1}/W \rangle}, \tag{4.25}$$

$$\langle \text{BER}_{d_2} \rangle = \frac{\sum_{r=1}^{R} \sum_{\substack{s=1 \\ s \neq R+1}}^{r+1} \sum_{i_{rs}^2} \overline{\text{BER}}_{rs}(i_{rs}^2) + \frac{1}{2} \sum_{i_{RR+1}^2} \overline{\text{BER}}_{RR+1}(i_{RR+1}^2)}{\langle R_{d_2}/W \rangle} \tag{4.26}$$

where

$$\overline{\text{BER}}_{BPSK} = \int_{\gamma_0}^{\gamma_1^1} \frac{1}{2} \text{erfc}(\sqrt{\gamma}) p_\gamma(\gamma) d\gamma, \tag{4.27}$$

$$\overline{\text{BER}}_{rs}(i_k/q_k) = \int_{\gamma_r^s}^{\gamma_r^{s+1}} P_b^{s/r}(M_r, \gamma, \mathbf{p}_{rs}^i, \mathbf{p}_{rs}^q, i_k/q_k) p_\gamma(\gamma) d\gamma, \tag{4.28}$$

i_{rs}^v, i_{rs}^1's and i_{rs}^2's are the assigned sub-channel positions of voice bit, Class-I data bits and Class-II data bits, respectively in s-th sub-region of r-th fading region. The integrals in (4.27) and (4.28) can be computed numerically. However, they can be evaluated in closed form for integer values of Nakagami fading parameter m as shown in the Appendix. The

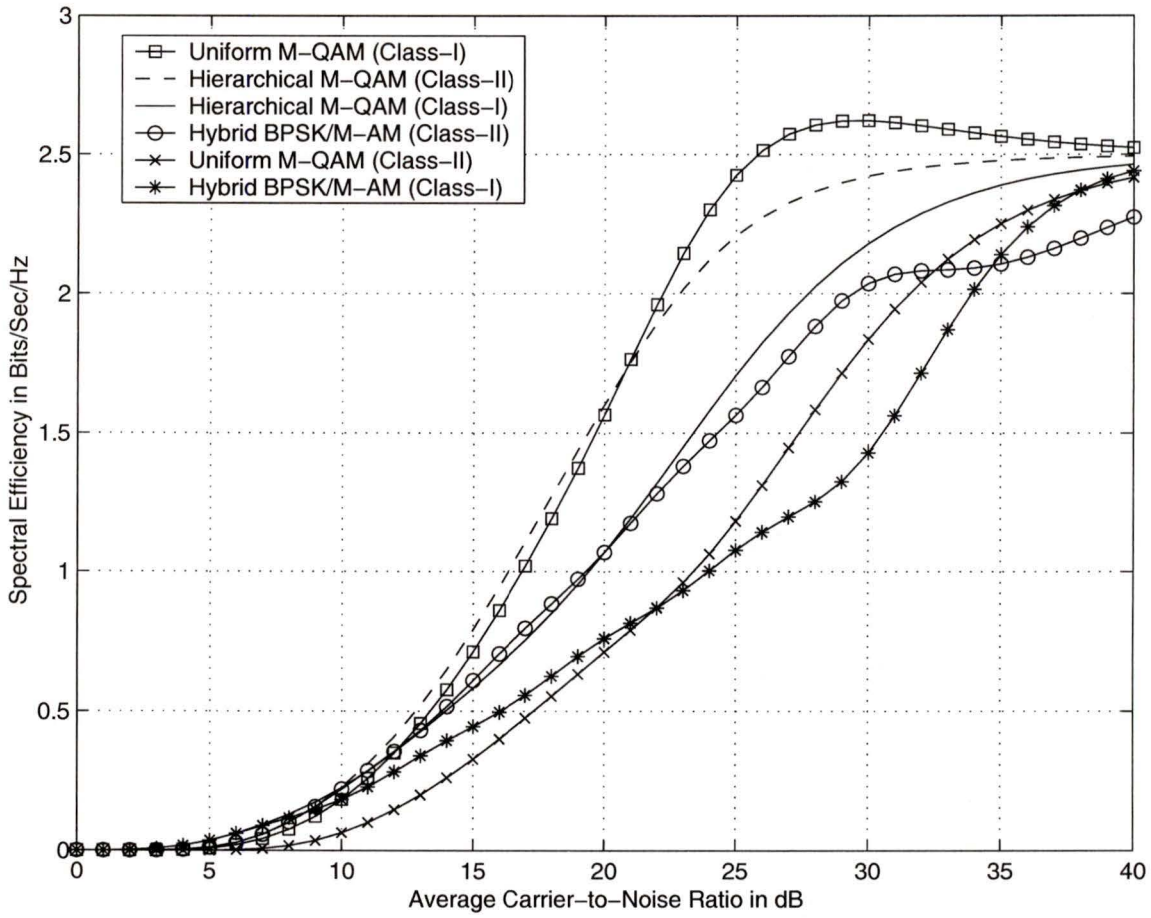

Figure 4.6. *Achievable spectral efficiency versus the average CNR $\bar{\gamma}$ in Rayleigh fading channel (m=1).*

average BERs for voice and different classes of data plotted in Fig. 4.9 show that the voice, Class-I and Class-II data are always sent below their respective target BERs as expected from our conservative choice of constellation size as well as the priority parameters. In addition, as the CNR increases the average BER increases for all kind of transmission since the schemes use the largest constellation often when the average CNR is high and the average BER prediction as $\bar{\gamma}$ increases becomes dominated by the BER of that constellation.

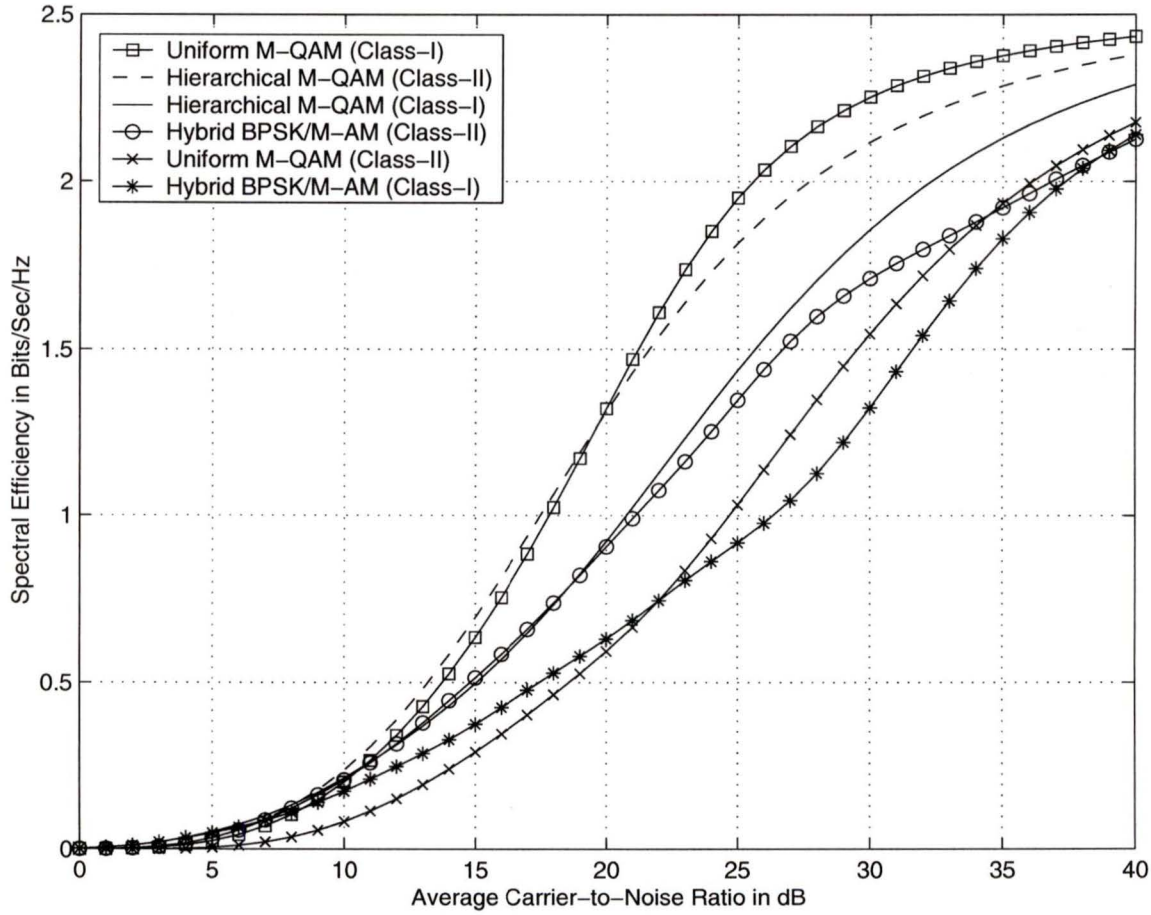

Figure 4.7. *Achievable spectral efficiency versus the average CNR $\bar{\gamma}$ (m=1/2).*

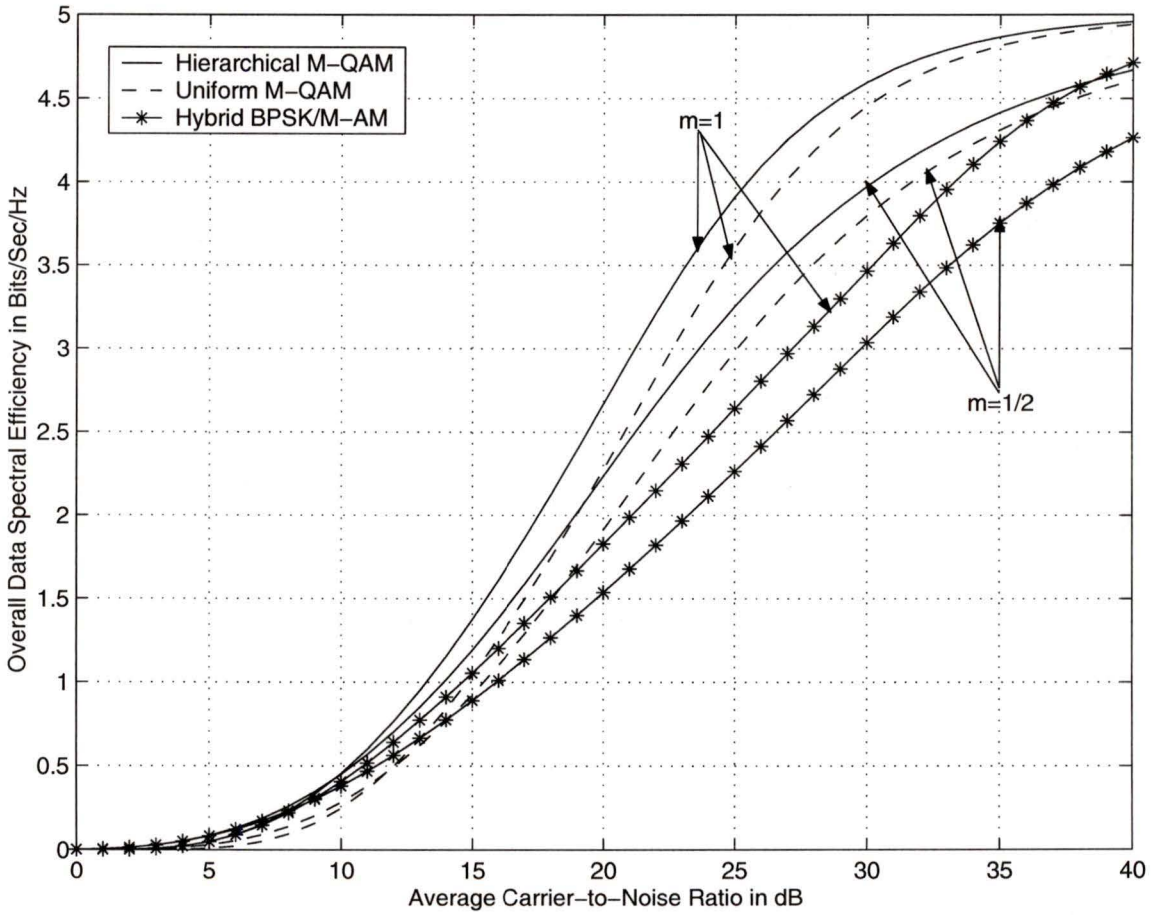

Figure 4.8. *Overall data spectral efficiency versus the average CNR* $\bar{\gamma}$.

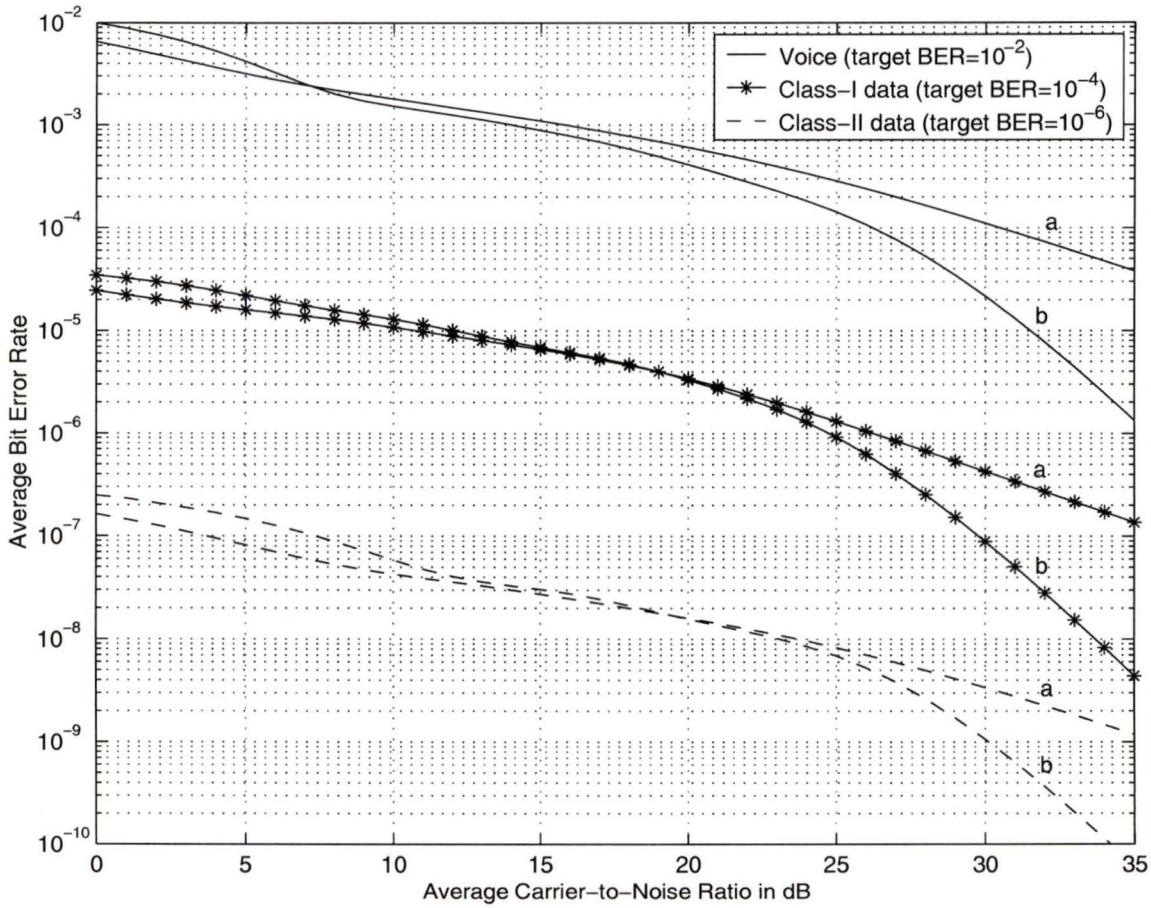

Figure 4.9. *Average BER versus the average CNR $\bar{\gamma}$: (a) $m = 1$, and (b) $m = 3$.*

4.2.2 Voice and Single Class Data Transmission

Simultaneous voice as well as single class data transmission can be considered as a special case of the voice and two different classes of data transmission when both classes of data require same BER i.e., $\text{BER}_{d_1} = \text{BER}_{d_2}$. Without loss of generality we consider the case of simultaneous voice and data transmission with a voice target BER, BER_v and a data target BER, BER_{d_1}. In this special case, the sub-region boundaries $\{\gamma_r^s\}_{s=1}^{r+1}$, in each fading region, become identical to the corresponding region boundary γ_r. Also the transmission parameters selected in first sub-region of a given region, r $(r = 1, 2, \cdots, R)$ remains same throughout the whole region, r. Therefore, only the region boundaries $\{\gamma_r\}_{r=1}^{R}$ are useful for simultaneous voice and single class data transmission. Specifically, the constellation size, M_r $(r = 1, 2 \cdots, R)$ is selected according to the switching thresholds $\{\gamma_r\}_{r=1}^{R+1}$. The voice bit is always transmitted in the LSB position of Q channel and Class-I data bits are transmitted in remaining r sub-channels. Therefore, the priority vectors in each region are selected such as the LSB sub-channel of the Q channel supports the voice below a target voice BER, BER_v while remaining r data sub-channels support data bits below a target data BER, BER_{d_1}.

4.2.2.1 Outage Probability

The outage probability for voice P_{out}^v is identical to (4.7) and the data outage probability P_{out}^d can be expressed as

$$\begin{aligned} P_{\text{out}}^d &= \int_0^{\gamma_1^1} p_\gamma(\gamma) d\gamma = \int_0^{\gamma_1} p_\gamma(\gamma) d\gamma \\ &= 1 - \frac{\Gamma\left(m, m\frac{\gamma_1}{\bar{\gamma}}\right)}{\Gamma(m)} \end{aligned} \tag{4.29}$$

The outage probability for voice transmission versus average CNR $\bar{\gamma}$ is same as the plot shown in Fig. 4.3. The data outage probability for data transmission is same as the Class-I data transmission outage probability as shown in Fig. 4.4. The adaptive hierarchical scheme offers the same outage probability for voice and data as the scheme employing

BPSK/M-AM which offers lower data outage than the scheme employing uniform M-QAM. The reason is described in Section 4.2.1.

4.2.2.2 Achievable Spectral Efficiency

The achievable spectral efficiency for voice transmission is identical to (4.13) while the spectral efficiency for data transmission $\langle R_d \rangle / W$ can be obtained by adding up (4.15) and (4.16). Specifically, data spectral efficiency $\langle R_d \rangle / W$ can be written as

$$\frac{\langle R_d \rangle}{W} = \frac{\langle R_{d_1} \rangle}{W} + \frac{\langle R_{d_2} \rangle}{W}. \tag{4.30}$$

Since $\{\gamma_r^s\}_{s=1}^{r+1} = \gamma_r$ (for $r = 1, 2, \cdots .R$), the probabilities $\{a_{rs}\}_{s=1}^{r+1}$ reduce to the probabilities that the CNR falls in the r-th region expressed as

$$a_r = \frac{\Gamma\left(m, m\frac{\gamma_r}{\bar{\gamma}}\right) - \Gamma\left(m, m\frac{\gamma_{r+1}}{\bar{\gamma}}\right)}{\Gamma(m)}; \quad r = 1, 2, \cdots, R. \tag{4.31}$$

Substituting $\{a_{rs}\}_{s=1}^{r+1} = a_r$ in (4.15) and (4.16), (4.30) can be expressed as

$$\frac{\langle R_d \rangle}{W} = \sum_{r=1}^{R} r a_r. \tag{4.32}$$

The achievable spectral efficiency for simultaneous voice and single class data transmission with three different schemes are plotted for different values of m in Figs. 4.10-4.11. These figures show that hierarchical QAM offers higher spectral efficiency for data transmission in medium and high CNR (above 10 dB) range than both the schemes in [17] and [18] while offering the same spectral efficiency as the scheme in [17] in low CNR region (upto 10dB) where the scheme in [18] suffers from low spectral efficiency.

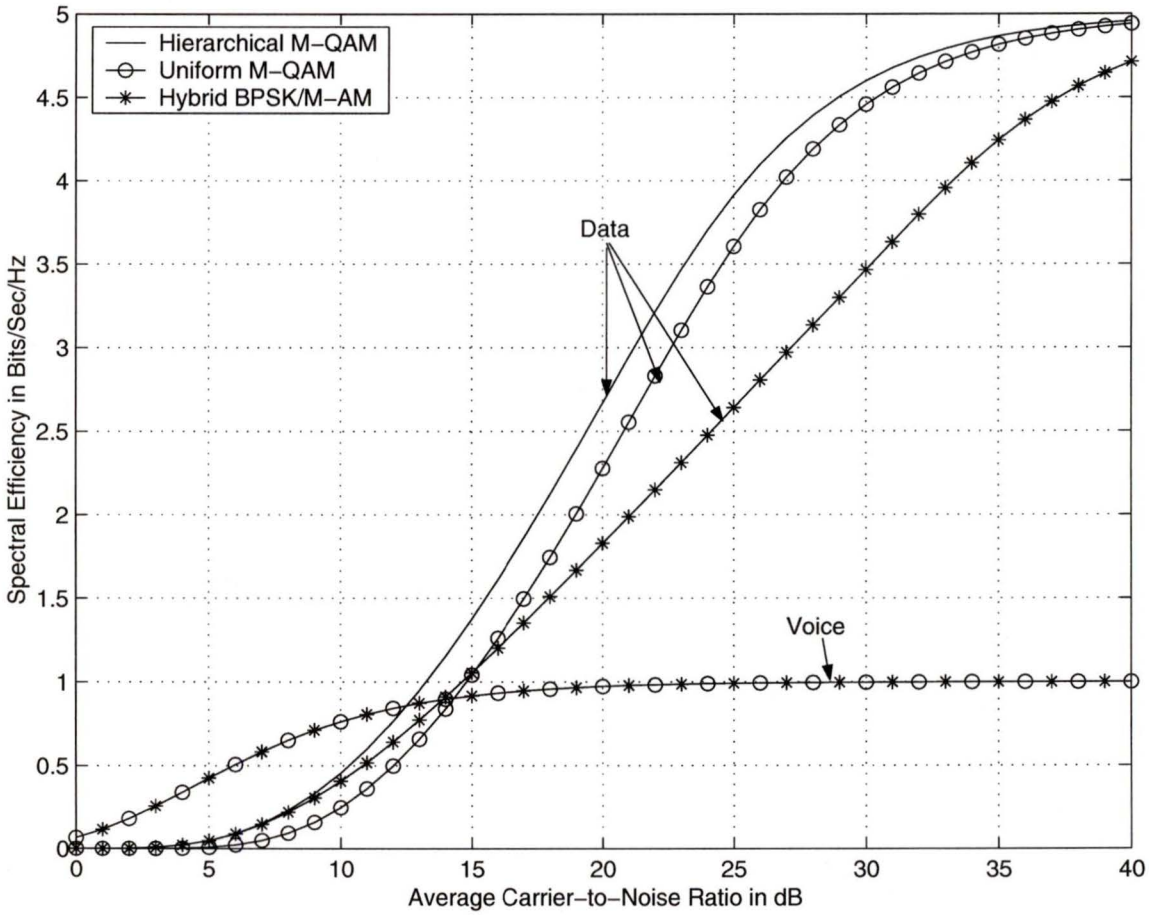

Figure 4.10. *Achievable spectral efficiency (for voice and single class data transmission) versus the average CNR* $\bar{\gamma}$ *(*$m = 1$*).*

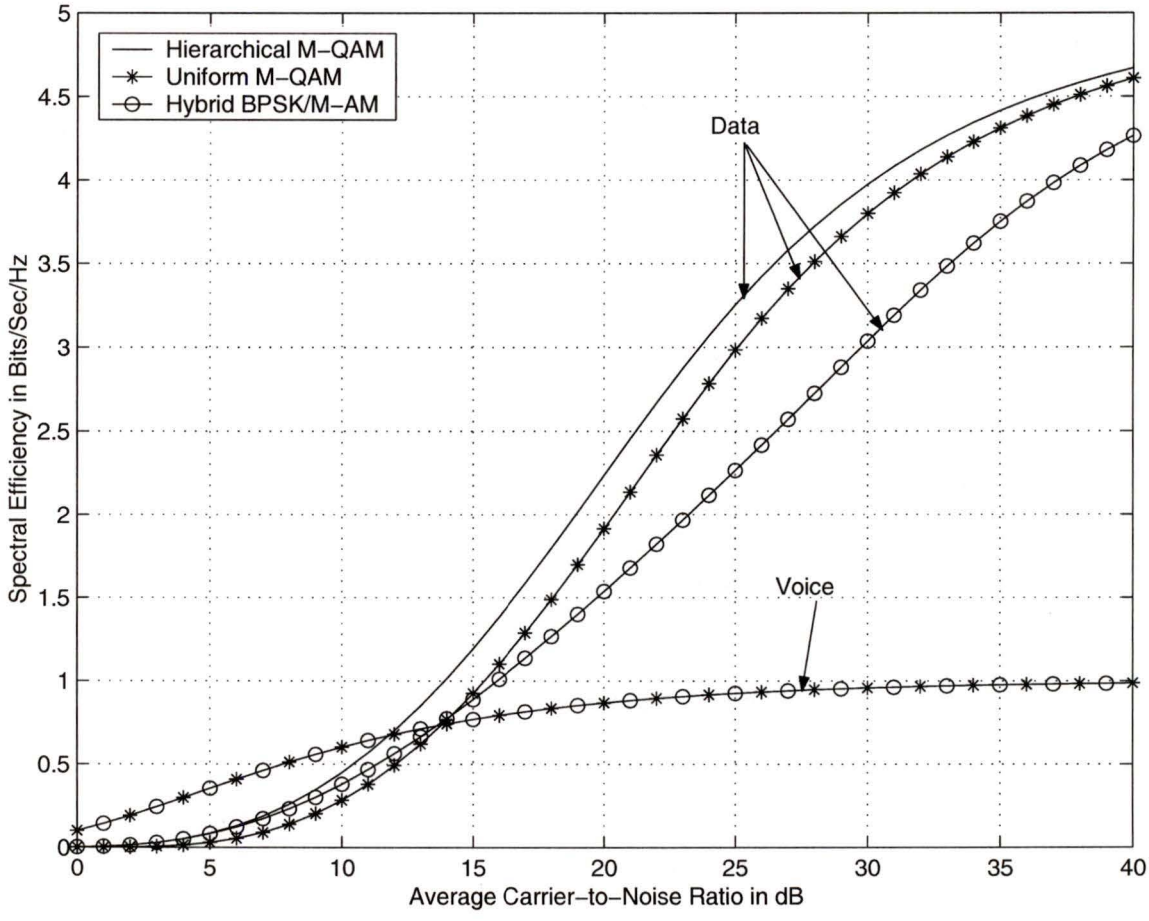

Figure 4.11. *Achievable spectral efficiency (for voice and single class data transmission) versus the average CNR* $\bar{\gamma}$ *(*$m = 1/2$*).*

4.2.2.3 Average BER

For single class data and voice transmission, the average BER for voice transmission $\langle \mathrm{BER}_v \rangle$ and data transmission $\langle \mathrm{BER}_d \rangle$ reduce to

$$\langle \mathrm{BER}_v \rangle = \frac{\overline{\mathrm{BER}}_{BPSK} + \sum_{r=1}^{R} \sum_{i_r^v} \overline{\mathrm{BER}}_r(i_r^v)}{\langle R_v/W \rangle}, \tag{4.33}$$

$$\langle \mathrm{BER}_d \rangle = \frac{\sum_{r=1}^{R} \sum_{i_r^d} \overline{\mathrm{BER}}_r(i_r^d)}{\langle R_d/W \rangle} \tag{4.34}$$

where

$$\overline{\mathrm{BER}}_r(i_k/q_k) = \int_{\gamma_r}^{\gamma_{r+1}} P_b^{s/r}(M_r, \mathbf{p}_r^i, \gamma, \mathbf{p}_r^q, i_k/q_k) p_\gamma(\gamma) d\gamma, \tag{4.35}$$

i_r^v and i_r^d's are the assigned sub-channel position to voice and data bit, respectively in r-th fading region. The average BERs for voice and data transmission are plotted in Fig. 4.12. The average BERs are below the their respective target BERs and decrease as the average CNR increases. This is again expected for the same reason mentioned in Section 4.2.1.

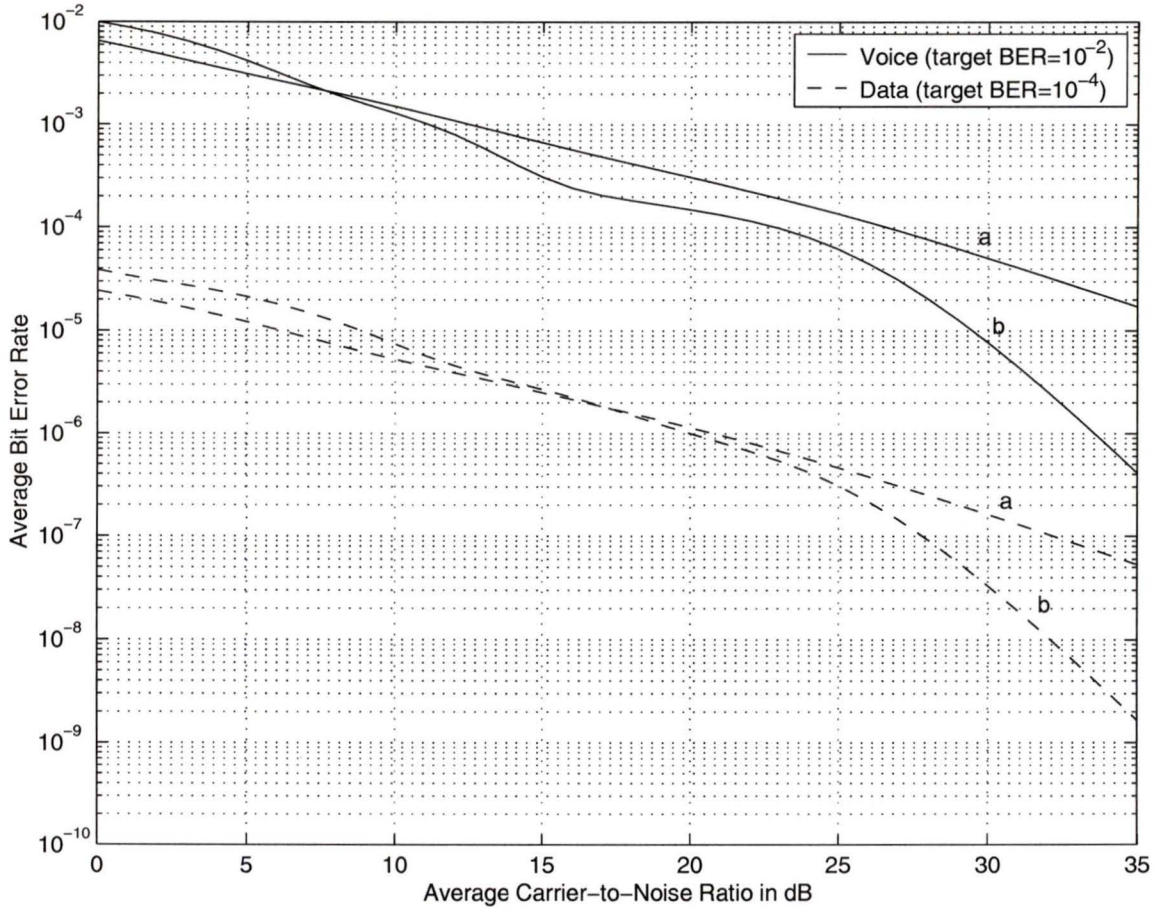

Figure 4.12. *Average BER (for voice and single class data transmission) versus the average CNR $\bar{\gamma}$: (a) $m = 1$, and (b) $m = 3$.*

Chapter 5

Conclusion

We have proposed multimedia and multicast transmission technique over slow fading channel using an adaptive hierarchical PSK constellation. Our proposed schemes, for both applications, have been compared with TDM that employs a uniform PSK. Simulation results show that the proposed schemes are more energy efficient than the uniform PSK in TDM. In multimedia transmission, the energy gain depends on the services transmitted. As the difference of BERs between different class of services increases, the gain also increases. The energy gain, in multicasting, depends on the recipients' link qualities as well as the quality of the multicasted message. Moreover, due to bit level multiplexing with hierarchical constellations, each service class of multimedia traffic transmits bits in each symbol. For the same reason, each recipient receives bits in each multicasted symbol with hierarchical PSK. So, different services and recipients do not experience the delay that is introduced in conventional TDM.

An adaptive technique employing hierarchical M-QAM constellation has been proposed as a link layer solution to simultaneous voice and different classes of data transmission problem over fading channels. We have also extended the schemes employing hybrid BPSK/M-AM and uniform M-QAM for simultaneous voice and two classes of data transmission. The anlytical results were able to clearly demonstrate that the proposed hierarchical scheme is spectrally more efficient for data transmission than the extended schemes. In addition, the hierachical scheme achieves better throughput fairness for both classes of data compared to other schemes under consideration which offer higher spectral efficiency

for one class of data at the cost of other. The hierarchical scheme is also an efficient way of transmitting simultaneously voice and single class data.

5.1 Suggestions for Further Work

There are number of interesting topics which may be pursued for the future work.

- Combine different error control coding techiques with the proposed schemes to increase the spectral efficiency.
- Generalization of downlink multiplexing problem with hierarchical constellations might be interesting. For example, we assumed that each recipient has same BER and data rate requirements. So, we ranked the recipients according to their link qualities and assigned different sub-channels to them accordingly. But if different recipients have different BER requirements with different data rates how the recipients can be ranked to assign them different sub-channels.
- Assign different sub-channels to different classes of data in simultaneous voice and different classes of data transmission such as the relative throughput of different classes of data can be controlled.
- Use of hierarchical constellations in automatic repeat request (ARQ) for multiresolution transmission and multimedia transmission with different delay requirements.

Bibliography

[1] A. J. Mueller, *Issues in Diversity and Adaptive Error Control Coding for Wireless Communications*, M.A.Sc. Thesis, University of Victoria, Victoria, Canada 1995.

[2] J. F. Hayes, "Adaptive feedback communications," *IEEE Transaction on Communication Technology*, vol. COM-16, pp. 29-34, Feb. 1968.

[3] J. K. Cavers, "Variable-rate transmission for Rayleigh fading channels," *IEEE Transaction on Communication Technology*, vol. COM-20, pp. 15-22, Feb. 1972.

[4] B. Vucetic, "An adaptive coding scheme for time-varying channels," *IEEE Transaction on Communications*, vol. COM-39, pp. 653-663, May 1991.

[5] S. Otsuki, S. Sampei and N. Morinaga, "Square-QAM adaptive modulation/TDMA/TDD systems using modulation level estimation with Walsh function," *Electron Letters*, vol. 31, pp. 169-171, Feb. 1995.

[6] W. T. Webb and R. Steele, "Variable rate QAM for mobile radio," *IEEE Transaction on Communications*, vol. COM-43, pp. 2223-2230, Jul. 1991.

[7] Y. Kamio, S. Sampei, S. Sasaoka and N. Morinaga, "Performance of modulation-level-controlled adaptive-modulation under limited transmission delay time for land mobile communications," in *Proc. IEEE Vehicular Technology Conference (VTC'95)*, Chicago, Illinois, Jul. 1995, pp. 221-225.

[8] J. M. Torrance and L. Hanzo, "Upper bound performance of adaptive modulation in a slow Rayleigh fading channel," *Electron Letters*, vol. 32, pp. 718-719, Apr. 1996.

[9] M.-S. Alouini and A. J. Goldsmith, "Adaptive M-QAM modulation over Nakagami fading channels," in *Proc. Communication Theory Mini Conference (CTMC-VI)* in conjunction with *IEEE Global Communication Conference (GLOBECOM'97)*, Phoenix, AZ, Nov. 1997, pp. 218-223.

[10] V. O. Hentine, "Error performance for adaptive transmission on fading channels," *IEEE Transaction on Communications*, vol. COM-22, pp. 1331-1337, Sept. 1974.

[11] A. J. Goldsmith and P. Varaiya, "Increasing spectral efficiency through power control," in *Proc. IEEE International Conference on Communications (ICC'93)*, Geneva, Switzerland, Jun. 1993, pp. 600-604.

[12] S. M. Alamouti and S. Kallel, "Adaptive trellis-coded multiple-phased-shift keying

for Rayleigh fading channels," *IEEE Transaction on Communications*, vol. COM-42, pp. 2305-2313, Jun. 1994.

[13] A. J. Goldsmith and S. G. Chua, "Adaptive coded modulation for fading channels," *IEEE Transaction on Communications*, vol. COM-46, pp. 595-602, May 1998.

[14] T. Ue, S. Sampei and N. Morinaga, "Symbol rate and modulation level controlled adaptive modulation/TDMA/TDD for personal communication systems," *IEICE Transaction on Communications*, vol. E78-B, pp. 1117-1124, Aug. 1998.

[15] H. Matsuoka, S. Sampei, N. Morinaga and Y. Kamio, "Adaptive modulation system with variable coding rate concatenated code for high quality multi-media communication systems," *IEICE Transaction Communications*, vol. E79-B, pp. 328-334, Mar. 1996.

[16] G. Bremer and K. D. Ko, "Simultaneous voice and data on the general switched telephone network using framed QADM," *IEEE Communication Magazine*, vol. 34, pp. 58-63, Dec. 1996.

[17] M.-S. Alouini, X. Tang and A. J. Goldsmith, "An adaptive modulation scheme for simultaneous voice and data transmission over fading channels," *IEEE Journal of Selected Areas in Communications*, vol. SAC-17, pp. 837-850, May 1999.

[18] C.-S. Hwang and Y. Kim, "An adaptive modulation for integrated voice/data traffic over Nakagami fading channels," in *Proc. IEEE Vehicular Technology Conference (VTC'2001-Fall)*, Atlantic City, NJ, Sept. 2001, pp. 1649-1652.

[19] D. J. Goodman, R. A. Valenzuela, K. T. Gayliard and B. Ramamurthi, "Packet reservation multiple multiple access for local wireless communications," *IEEE Transaction on Communications*, vol. COM-37, pp. 885-890, Aug. 1989.

[20] K. Zhang and K. Pahlavan, "An integrated voice/data system for mobile indoor radio networks," *IEEE Transaction on Vehicular Technology*, vol. VT-39, pp. 75-82, Feb. 1990.

[21] S. Nanda, "Analysis of packet reservation multiple access: Voice data integration for wireless networks," in *Proc. IEEE Global Communication Conference (GLOBECOM'90)*, San Diego, CA, Dec. 1990, pp. 1984-1988.

[22] N. Wilson, R. Ganesh, K. Joseph and D. Raychaudhuri, "Packet CDMA versus dynamic TDMA for multiple access in an integrated voice/data PCN," *IEEE Journal of Selected Areas in Communications*, vol. SAC-11, pp. 870-884, Aug. 1993.

[23] G. Wu, K. Mukumoto and A. Fukud, "Analysis of an integrated voice and data transmission system using packet reservation multiple access," *IEEE Transaction on Vehicular Technology*, vol. VT-43, pp. 289-297, May 1994.

[24] B. C. Kim and C. K. Un, "An efficient wireless voice/data integrated access algorithm in noisy channel environments," *IEICE Transaction on Communications*, vol. E79-B, pp. 1394-1403, Sept. 1996.

[25] M. Nakagami, "The m-distribution–A general formula of intensity distribution of rapid fading," in *Statistical Methods in Radio Wave Propagation*, Oxford, UK: Pergamon, 1960, pp. 3-36.

[26] I. S. Gradshteyn and I. M. Ryzhik, *Table of Integrals, Series, and Products*, 5th ed. San Diego, CA: Academic, 1994.

[27] C. E. W. Sundberg, W. C. Wong and R. Steele, "Logarithmic PCM weighted QAM transmission over Gaussian and Rayleigh fading channels," *IEEE Proc.,* vol. 134, pp. 557-570, Oct. 1987.

[28] K. Ramchandran, A. Ortega, K. M. Uz and M. Vetterli, "Multiresolution broadcast for digital HDTV using joint source/channel coding," *IEEE Journal of Selected Areas in Communications,* vol. 11, no. 1, pp. 6-23, Jan. 1993.

[29] L.-F. Wei, "Coded modulation with unequal error protection," *IEEE Transaction on Communications,* vol. 41, no. 10, pp. 1439-1449, Oct. 1993.

[30] M. Morimoto, H. Harada, M. Okada and S. Komaki, "A study on power assignment of hierarchical modulation schemes for digital broadcasting," *IEICE Transactions on Communications*, vol. E77-B, pp. 1495-1500, Dec. 1994.

[31] M. Morimoto, M. Okada and S. Komaki, "A hierarchical image transmission system in a fading channel," *IEEE International Conference on Universal Personal Communications (ICUPC'95),* Tokyo, Japan, Nov. 1995, pp. 769-772.

[32] M. B. Pursley and J. M. Shea, "Nonuniform phase-shift-key modulation for multimedia multicast transmission in mobile wireless networks," *IEEE Journal of Selected Areas in Communications,* vol. SAC-17, pp. 774-783, May 1999.

[33] M. B. Pursley and J. M. Shea, "Adaptive nonuniform phase-shift-key modulation for multimedia traffic in wireless networks.," *IEEE Journal of Selected Areas in Communications,* vol. SAC-18, pp. 1394-1407, Aug. 2000.

[34] DVB-T standard: ETS 300 744., "*Digital Broadcasting Systems for Television, Sound and Data Services: Framing Structure, Channel Coding and Modulation for Digital Terrestrial Television,*" (ETS Draft, 1.2.1, EN300 744, 1999-1).

[35] P. K. Vitthaladevuni and M.-S. Alouini, "A recursive algorithm for the exact BER computation of generalized hierarchical QAM constellations," *IEEE Transactions on Information Theory,* vol. IT-49, pp. 297-307, Jan. 2003.

[36] P. K. Vitthaladevuni and M.-S. Alouini, "Exact BER computation of generalized

hierarchical PSK constellations" in *Proc. IEEE International Conference on Communications (ICC'02)*, New York city, NY, Apr.-May 2002, pp. 1974 -1978.

[37] P. K. Vitthaladevuni and M.-S. Alouini, "Effect of imperfect phase and timing synchronization on the error rate performance of PSK modulations," in *Proc. IEEE Vehicular Technology Conference (VTC'02 Fall),* Vancouver, Canada, Sept. 2002, pp. 356 -360, Journal version submitted to *IEEE Transaction on Communications.*

[38] P. K. Vitthaladevuni and M.-S. Alouini, "A closed-form expressions for the exact BER of generalized QAM constellations," in *Proc. 5th Nordic Signal Processing Symposium (NORSIG),* Trondheim, Norway, Oct. 2002, Journal version submitted to *IEEE Transaction on Communications*.

[39] R. F. Pawula, S. O. Rice and J. H. Roberts, "Distribution of the phase angle between two vectors perturbed by Gaussian noise," *IEEE Transaction on Communications,* vol. COM-30, pp. 1828-1841, Aug. 1982.

[40] J. Kim, I. Kim, S. Ro, D. Hong and C. Kang, "Effects of multipath diversity on adaptive QAM in frequency selective Rayleigh fading channels," *IEEE Communication Letter*, vol. 6, pp. 364-366, Sept. 2002.

Appendix A

Average BER

In this Appendix. we show that the integrals in (4.27) and (4.28) can be evaluated in closed form for integer values of Nakagami fading parameter m.

The BER expressions for M-QAM over AWGN channel are in the form of a weighted sum of complementary error functions and are solely dependent on the constellation size M, the carrier-to-noise ratio γ, and priority parameters $\mathbf{p}^i$ and $\mathbf{p}^q$. The instantaneous BER of inphase bits in hierarchical M-QAM constellation over AWGN channel can be written as [38]

$$P_b^{s/r}(M, \mathbf{p}^i, \mathbf{p}^q, \gamma, i_k) = \sum_j \left[A_j + B_j \left[\sum_l D_l \text{erfc}(a_{jl}\sqrt{\gamma}) \right] \right], \quad \text{for} \quad i_k = 1, 2, \cdots, y, \tag{A.1}$$

where constant A_j, B_j and D_l depend on M and i_k and constant a_{jl} depends on M, $\mathbf{p}^i$, $\mathbf{p}^q$ and i_k. Inspired by the result in [40], we derive the average BER of i_kth $(i_k = 1, 2, \cdots, y)$ position bit in the inphase channel of constant power hierarchical QAM in sth subregion of rth region over Nakagami fading channel as follows:

$$\overline{\text{BER}}_{rs}(\bar{\gamma}, i_k) = \int_{\gamma_r^s}^{\gamma_r^{s+1}} f_I(M_r, \mathbf{p}_{rs}^i, \mathbf{p}_{rs}^q, \gamma, i_k) p_\gamma(\gamma) d\gamma. \tag{A.2}$$

Using (A.1), we can write

$$\overline{\text{BER}}_{rs}(\bar{\gamma}, i_k) = \sum_j \left[A_j \int_{\gamma_r^s}^{\gamma_r^{s+1}} p_\gamma(\gamma) d\gamma + B_j \left[\sum_l D_l \int_{\gamma_r^s}^{\gamma_r^{s+1}} \text{erfc}(a_{jl}\sqrt{\gamma}) p_\gamma(\gamma) d\gamma \right] \right]. \tag{A.3}$$

Let us consider

$$I = \int \text{erfc}(a_{jl}\sqrt{\gamma}) p_\gamma(\gamma) d\gamma. \tag{A.4}$$

For integer values of Nakagami fading parameter m, using (2.3) and integrating by parts, we get

$$I = \text{erfc}(a_{jl}\sqrt{\gamma}) I_1 - I_2 \tag{A.5}$$

where

$$I_1 = \int \left(\frac{m}{\bar{\gamma}}\right)^m \frac{\gamma^{m-1}}{\Gamma(m)} \exp\left(-m\frac{\gamma}{\bar{\gamma}}\right) d\gamma \tag{A.6}$$

$$= -\sum_{n=0}^{m-1} \frac{1}{n!} \left(\frac{m\gamma}{\bar{\gamma}}\right)^n \exp\left(\frac{-m\gamma}{\bar{\gamma}}\right). \tag{A.7}$$

and

$$I_2 = \int \frac{d}{d\gamma}[\text{erfc}(a_{jl}\sqrt{\gamma})] I_1 d\gamma \tag{A.8}$$

$$= -\sum_{n=0}^{m-1} \frac{1}{n!} \int \frac{d}{d\gamma}[\text{erfc}(a_{jl}\sqrt{\gamma})] \left(\frac{m\gamma}{\bar{\gamma}}\right)^n \exp\left(\frac{-m\gamma}{\bar{\gamma}}\right) d\gamma \tag{A.9}$$

Since

$$\frac{d}{d\gamma}[\text{erfc}(a_{jl}\sqrt{\gamma})] = -\frac{a_{jl}}{\sqrt{\pi}} \gamma^{-1/2} e^{-(a_{jl}^2\gamma)}, \tag{A.10}$$

I_2 becomes

$$I_2 = \sum_{n=0}^{m-1} \frac{1}{n!} \left(\frac{m}{\bar{\gamma}}\right)^n \frac{a_{jl}}{\sqrt{\pi}} \int \gamma^{n-\frac{1}{2}} e^{-(a_{jl}^2 + \frac{m}{\bar{\gamma}})\gamma} d\gamma. \tag{A.11}$$

Using (A.7) and (A.11) in (A.3), we get the desired closed-form result

$$\begin{aligned} \overline{\text{BER}}_{rs}(\bar{\gamma}, i_k) = \sum_j \Bigg\{ \Bigg[& A_j \sum_{n=0}^{m-1} \frac{1}{n!} \left(\frac{m\gamma}{\bar{\gamma}}\right)^n \exp\left(-\frac{m\gamma}{\bar{\gamma}}\right) \\ & + B_j \Bigg[\sum_l D_l \Bigg[\text{erfc}(a_{jl}\sqrt{\gamma}) \sum_{n=0}^{m-1} \frac{1}{n!} \left(\frac{m\gamma}{\bar{\gamma}}\right)^n \exp\left(-\frac{m\gamma}{\bar{\gamma}}\right) \\ & - \sum_{n=0}^{m-1} \frac{1}{n!} \frac{a_{jl}}{\sqrt{\pi}} \mu^{-(n+\frac{1}{2})} \times \Gamma(n+\frac{1}{2}, \mu\gamma) \Bigg] \Bigg] \Bigg] \Bigg\}_{\gamma_r^{s+1}}^{\gamma_r^s} \end{aligned} \tag{A.12}$$

where $\mu = (a_{jl}^2 + \frac{m}{\bar{\gamma}})$. Similarly, the average BER of different position bits in the Q phase channel can be evaluated in closed-form for integer values of m.

VITA

Surname: Hossain ***Given Names:*** Md. Jahangir

Place of Birth: Jhenaidah, Bangladesh

Educational Institutions Attended

Bangladesh University of Engineering and Technology	1995 to 2000

Degrees Awarded

B.Sc. Eng.	Bangladesh University of Engineering and Technology	2000

Honors and Awards

Petch Research Scholarship, Canada	2002-2003
University of Victoria Fellowship, Canada	2002-2003
Altaf Hossain Memorial Fellowship, Bangladesh	1999-2000
University Merit Scholarships, Bangladesh	1995-2000

Journal Publications

1. Md. J. Hossain, P. K. Vitthaladevuni, M.-S. Alouini, V. K. Bhargava and A. J. Goldsmith, "Adaptive Hierarchical Modulation for Simultaneous Voice and Multi-Class Data Transmission over Fading Channels," submitted to *IEEE Transaction on Wireless Communications*, August 2003.
2. Md. K. Hasan, Md. J. Hossain and M. A. Haque, "Parameter Estimation of Multichannel Autoregressive Processes in Noise," *Signal Processing*, Elsevier Science, vol. 83, pp. 603-610, March 2003.

Conference Publications

1. Md. J. Hossain, P. K. Vitthaladevuni, M.-S. Alouini, V. K. Bhargava and A. J. Goldsmith, "Adaptive Hierarchical Modulation for Simultaneous Voice and Multi-Class Data Transmission over Fading Channels," to appear in *Proc. IEEE IV Workshop on Signal Processing Advances in Wireless Communication*, Rome, Italy, June 15-18, 2003.

2. Md. J. Hossain, P. K. Vitthaladevuni, M.-S. Alouini and V. K. Bhargava, "Hierarchical Constellations for Multimedia and Multicast Transmission over Fading Channels," in *Proc. IEEE Vehicular Technology Conference (VTC'03) Spring*, April 2003, Jeju Island, Korea, pp. 2633-2637.

3. P. K. Vitthaladevuni, Md. J. Hossain, M.-S. Alouini and V. K. Bhargava, "Hierarchical Constellations for Multimedia Transmission over Fading Channels," in *Proc. 14th Annual Transportation Research Conference (TRC'2003)*, Minneapolis, MN, Apr. 2003, pp. 21.

4. Md. J. Hossain and Md. K. Hasan, "Multichannel Autoregressive Spectral Estimation from Noisy Observations," in *Proc. IEEE TENCON'00*, Kuala Lumpur, Malaysia, Sept. 2000, pp. 327-332.

UNIVERSITY OF VICTORIA PARTIAL COPYRIGHT LICENSE

I hereby grant the right to lend my thesis to users of the University of Victoria Library, and to make single copies only for such users or in response to a request from the Library of any other university, or similar institution, on its behalf or for one of its users. I further agree that permission for extensive copying of this thesis for scholarly purposes may be granted by me or a member of the University designated by me. It is understood that copying or publication of this thesis for financial gain by the University of Victoria shall not be allowed without my written permission.

Title of Thesis:

Applications of Hierarchical Constellations for Multimedia Transmission over Fading Channels

Author: 

MD. JAHANGIR HOSSAIN
August 11, 2003